Plant Physiology®

Research Article

BnaABF3 and BnaMYB44 regulate the transcription of zeaxanthin epoxidase genes in carotenoid and abscisic acid biosynthesis

Shenhua Ye [ID],[1,2] Yingying Huang,[1] Tiantian Ma,[1] Xiaowei Ma [ID],[1] Rihui Li [ID],[1] Jinxiong Shen [ID],[1] Jing Wen [ID][1,*]

1 National Key Laboratory of Crop Genetic Improvement, College of Plant Science and Technology, National Center of Rapeseed Improvement in Wuhan, Huazhong Agricultural University, Wuhan 430070, China

2 The Key Laboratory for Quality Improvement of Agricultural Products of Zhejiang Province, College of Advanced Agricultural Sciences, Zhejiang A&F University, Hangzhou 311300, China

*Author for correspondence: wenjing@mail.hzau.edu.cn
The author responsible for distribution of materials integral to the findings presented in this article in accordance with the policy described in the Instructions for Authors (https://academic.oup.com/plphys/pages/General-Instructions) is: Jing Wen (wenjing@mail.hzau.edu.cn).

Abstract

Zeaxanthin epoxidase (ZEP) is a key enzyme that catalyzes the conversion of zeaxanthin to violaxanthin in the carotenoid and abscisic acid (ABA) biosynthesis pathways. The rapeseed (Brassica napus) genome has 4 ZEP (BnaZEP) copies that are suspected to have undergone subfunctionalization, yet the 4 genes' underlying regulatory mechanisms remain unknown. Here, we genetically confirmed the functional divergence of the gene pairs BnaA09.ZEP/BnaC09.ZEP and BnaA07.ZEP/BnaC07.ZEP, which encode enzymes with tissue-specific roles in carotenoid and ABA biosynthesis in flowers and leaves, respectively. Molecular and transgenic experiments demonstrated that each BnaZEP pair is transcriptionally regulated via ABA-responsive element–binding factor 3 s (BnaABF3s) and BnaMYB44s as common and specific regulators, respectively. BnaABF3s directly bound to the promoters of all 4 BnaZEPs and activated their transcription, with overexpression of individual BnaABF3s inducing BnaZEP expression and ABA accumulation under drought stress. Conversely, loss of BnaABF3s function resulted in lower expression of several genes functioning in carotenoid and ABA metabolism and compromised drought tolerance. BnaMYB44s specifically targeted and repressed the expression of BnaA09.ZEP/BnaC09.ZEP but not BnaA07.ZEP/BnaC07.ZEP. Overexpression of BnaA07.MYB44 resulted in increased carotenoid content and an altered carotenoid profile in petals. Additionally, RNA-seq analysis indicated that BnaMYB44s functions as a repressor in phenylpropanoid and flavonoid biosynthesis. These findings provide clear evidence for the subfunctionalization of duplicated genes and contribute to our understanding of the complex regulatory network involved in carotenoid and ABA biosynthesis in B. napus.

Introduction

Carotenoids are natural pigments that give flowers and fruits colors ranging from yellow to red (Tanaka et al. 2008). These pigments play a pivotal role in essential bioprocesses in plants, such as photosynthesis, photoprotection, and antioxidant defense, and serve as precursors for the biosynthesis of abscisic acid (ABA) and strigolactones (Rodriguez-Concepcion et al.

2018). In the past few decades, the carotenoid biosynthetic pathway has been well characterized and is considered to be relatively conserved across plant species (Sun et al. 2018; Stanley and Yuan 2019). Carotenoid biosynthesis starts with the production of phytoene, which is catalyzed by phytoene synthase (PSY). Phytoene is further desaturated and isomerized to trans-lycopene by the sequential activity of phytoene

desaturase (PDS), ζ-carotene isomerase (Z-ISO), ζ-carotene desaturase, and carotenoid isomerase. At this point, the pathway bifurcates into the α- and β-carotene branches, leading to the production of lutein and violaxanthin, respectively. Major enzymes in the α-carotene branch include lycopene β-cyclase (LCYB), lycopene ε-cyclase, β-carotene hydroxylase (CYP97A3), and ε-carotenoid hydroxylase (CYP97C1), and in the β-carotene branch, LCYB, β-carotenoid hydroxylase 1 (BCH1), BCH2, zeaxanthin epoxidase (ZEP), and violaxanthin de-epoxidase (VDE). Carotenoid biosynthesis is mainly modulated through the transcriptional regulation of the above structural genes by transcription factors (TFs). Several TFs that directly regulate carotenoid biosynthesis have been documented in different species. For instance, the basic-helix-loop-helix TF PHYTOCHROME-INTERACTING FACTOR1 (PIF1) and the basic leucine zipper (bZIP) TF LONG HYPOCOTYL5 (HY5) targets *PSY* in Arabidopsis (*Arabidopsis thaliana*), MADS6 targets *LCYB1* in *Citrus sinensis*, and White petal1 (WP1) targets *LYCB* in *Medicago truncatula* (Toledo-Ortiz et al. 2014; Lu et al. 2018; Meng et al. 2019). Despite these discoveries, the transcriptional regulatory networks responsible for carotenoid biosynthesis remain largely unknown.

ABA plays a crucial role in plant development and acclimation to multiple stresses. Numerous genes involved in ABA biosynthesis and signaling pathways have been extensively studied (Nambara and Marion-Poll 2005; Chen et al. 2020). The initial reaction in ABA biosynthesis is catalyzed by ZEP, which is also responsible for the conversion of zeaxanthin to violaxanthin in carotenoid biosynthesis (Hieber et al. 2000; Nambara and Marion-Poll 2005). The role of *ZEP* in carotenoid biosynthesis, ABA biosynthesis, and drought stress tolerance has been thoroughly explored (Marin et al. 1996; Agrawal et al. 2001; Barrero et al. 2005; Galpaz et al. 2008; Lee et al. 2021). However, these studies were mostly limited to species with a single copy of *ZEP* in their genomes. The function of duplicated *ZEP*s in polyploids, and the regulatory network controlling their transcription, is far from understood. Furthermore, TFs from the family of ABA-responsive element (ABRE)-binding proteins/ABRE-binding factors (ABFs), especially ABF3, have been reported to be pivotal regulators of ABA signaling by modulating the expression of ABA-responsive genes (Yoshida et al. 2014; Chen et al. 2020). However, the target genes of ABF3 remain to be explored.

Polyploidization, which results in gene duplication, contributes substantially to species diversity and evolution (Moore and Purugganan 2005). Studying the fate of duplicated genes helps us to better understand how gene duplication shapes adaptive evolution (Flagel and Wendel 2009). Subfunctionalization is a relatively common fate of duplicated genes in plants, resulting in the protein functions or expression patterns of an ancestral gene being shared or divided by duplicated genes (Force et al. 1999; Panchy et al. 2016). In general, differential expression of duplicated genes is often attributed to the divergence of their regulatory cis-elements (Chaudhary et al. 2009; Zou et al. 2009; Hu et al. 2012;

Arsovski et al. 2015). Several studies have highlighted the existence of duplicates among carotenoid pathway genes, with each duplicated gene generally exhibiting a tissue-specific expression pattern, as shown for *PSY*, *LCYB*, and *BCH* in tomato and for *ZEP* and *carotenoid cleavage dioxygenase 4* (*CCD4*) in *Brassica napus* (Galpaz et al. 2006; Zhang et al. 2015; Liu et al. 2020). Whereas subfunctionalization of duplicated genes is prevalent in plants, there are still gaps in our understanding of how this process occurs, including the specific changes in gene regulation that allow for the tissue-specific expression of duplicated genes.

B. napus is a polyploid species formed by interspecific hybridization between *B. rapa* and *B. oleracea*. We previously showed that *B. napus* carries 4 *BnaZEP* copies, with the 2 genes from each pair (*BnaA09.ZEP/BnaC09.ZEP* and *BnaA07.ZEP/BnaC07.ZEP*) showing similar tissue-specific expression patterns, suggesting that *BnaZEP*s have undergone subfunctionalization (Liu et al. 2020). However, the functions of these *BnaZEP*s have not been investigated in detail, and the regulatory mechanism underlying their similar (within pairs) and distinct (across pairs) expression patterns remains elusive. Here, we genetically demonstrated the functional divergence of the 2 *BnaZEP* duplicated pairs, which can be attributed to variation in their cis-regulatory elements. Furthermore, we identified the ABA-inducible TFs BnaABF3s as positive regulators of the expression of the 4 *BnaZEP*s. Interestingly, BnaMYB44s were explored as TFs that regulate carotenoid accumulation in petals by specifically repressing the expression of *BnaA09.ZEP/BnaC09.ZEP*, highlighting another regulatory layer that contributes to the functional divergence of *BnaZEP*s. These findings provide a clear case of subfunctionalization for duplicated genes in polyploids and offer insights into the regulatory networks in carotenoid and ABA biosynthesis.

Results

BnaZEPs exhibit functional divergence and partial redundancy for carotenoid and ABA biosynthesis

We previously showed that the simultaneous knockout of *BnaA09.ZEP* and *BnaC09.ZEP* in *B. napus* led to a change in flower color from yellow to orange (Liu et al. 2020). To explore the function of *BnaA09.ZEP/BnaC09.ZEP* in carotenoid biosynthesis, we conducted ultra-performance liquid chromatography-tandem MS analysis of petals from orange-flowering O271 (carrying the nonfunctional alleles *Bnaa09.zepBnac09.zep*) and its yellow-flowering transgenic complementary lines harboring *BnaA09.ZEPpro:BnaA09.ZEP* (APSP line) or *BnaC09.ZEPpro:BnaC09.ZEP* (CPSP line), (Supplementary Fig. S1A). We determined that the yellow petals from APSP and CPSP have highly similar carotenoid contents and profiles, with substantially decreased carotenoid levels in comparison with the orange petals of O271. Compared with orange petals, yellow petals accumulated less zeaxanthin and antheraxanthin, showing decreased

contents by 88.7% to 91.5% and 84.9% to 88.3%, respectively. By contrast, violaxanthin levels were 80.3% and 109.5% higher in yellow petals than in orange petals. These results suggest that *BnaA09.ZEP* and *BnaC09.ZEP* encode functionally redundant enzymes for the conversion of zeaxanthin to antheraxanthin and subsequently to violaxanthin. Notably, we detected a small amount of violaxanthin (11.53 ± 0.29 μg/g) in orange petals, suggesting a partial functional compensation between *BnaA07.ZEP/BnaC07.ZEP* and *BnaA09.ZEP/BnaC09.ZEP* for carotenoid biosynthesis. Subcellular localization analysis showed that all 4 BnaZEP proteins localize to chloroplasts (Supplementary Fig. S1B), suggesting that BnaZEPs have similar subcellular locations and similar functions in different tissues of *B. napus*.

To further investigate the function of *BnaZEPs*, 2 clustered regularly interspaced short palindromic repeats (CRISPR)/CRISPR-associated 9 (Cas9) vectors were constructed and transformed into yellow-flowering *B. napus* var. Westar. One vector targeted *BnaA07.ZEP* and *BnaC07.ZEP*, while the other targeted all 4 *BnaZEPs* (Supplementary Fig. S2A). Two homozygous T$_2$ double mutants (*Bnaa07c07zep*) and 2 quadruple mutants (*Bnazeps*) were used for subsequent analyses (Supplementary Fig. S2B). In these lines, all the target alleles were null and exhibited premature translation termination. When grown in the field, no clear phenotypic differences were observed between *Bnaa09c09zep* (Liu et al. 2020) and Westar at the seedling stage. *Bnaa07c07zep* exhibited chlorotic young leaves, whereas *Bnazeps* displayed dwarfism and severe ABA-deficient phenotypes with yellow-wilted leaves (Fig. 1A). At the flowering stage, *Bnazeps* produced orange flowers that were darker than those of *Bnaa09c09zep*, whereas the flower color of *Bnaa07c07zep* remained yellow. When grown in the greenhouse, no clear phenotypic differences were observed among Westar, *Bnaa09c09zep*, and *Bnaa07c07zep* at the seedling stage. In agreement with the field data, *Bnazeps* had a dwarf stature and a severely wilted phenotype (Supplementary Fig. S3A). Compared with Westar, the ABA levels of *Bnazeps* were significantly lower, accompanied by greater stomatal aperture and density (Supplementary Fig. S3, B to E). Importantly, only continuous exogenous application of ABA could rescue the wilted phenotype of *Bnazeps* and ensure their survival (Fig. 1B).

To evaluate the role of BnaZEPs in ABA biosynthesis and drought tolerance, we withheld irrigation of 4-wk-old Westar, *Bnaa09c09zep*, and *Bnaa07c07zep* plants for 14 d before rewatering them. The survival rate of *Bnaa09c09zep* (34.4% on average) was not significantly different from that of Westar (39.2% on average). However, *Bnaa07c07zep* had a significantly lower survival rate (21.5% on average) than Westar and *Bnaa09c09zep* (Fig. 1, C and D), indicating that *Bnaa07c07zep* plants are more sensitive to drought stress. We also investigated the contents of malondialdehyde (MDA) and proline in these lines under well-watered and drought conditions (Fig. 1, E and F). Westar, *Bnaa09c09zep*, and *Bnaa07c07zep* produced nearly equal and relatively low amounts of proline and MDA under well-watered conditions; by contrast, under drought conditions, *Bnaa07c07zep* accumulated significantly less proline but

more MDA than Westar and *Bnaa09c09zep*. Subsequently, the ABA contents were investigated. All well-watered plants have very similar ABA contents (Fig. 1G). Drought stress promoted ABA production in all genotypes, although to a lesser extent in *Bnaa07c07zep* than in Westar and *Bnaa09c09zep*. Overall, these results showed that *BnaA09.ZEP* and *BnaC09.ZEP* are mainly responsible for flower color, whereas BnaA07.ZEP and BnaC07.ZEP mainly function in leaves, where they are involved in ABA production and drought tolerance. To a certain extent, the 2 pairs of *BnaZEPs* function in different tissues but also exhibit some functional redundancy in terms of carotenoid and ABA biosynthesis.

Variations in promoter sequences play important roles in the functional divergence of *BnaZEPs*

The genomic sequences of the 2 pairs of *BnaZEPs* showed highly similar coding sequences (CDSs; Liu et al. 2020) but substantial divergence in the 5′ noncoding sequences (Supplementary Fig. S4), suggesting that cis-regulation played an important role in the functional divergence of *BnaZEPs*. To test this possibility, we employed a promoter-swapping strategy in orange-flowering O271 (genotype: *Bnaa09c09zep*). We amplified the promoters of *BnaA09.ZEP* and *BnaC09.ZEP* and cloned them upstream of the CDSs of *BnaA07.ZEP* and *BnaC07.ZEP*, respectively. The resulting 2 promoter swap constructs were individually transformed into O271. A phenotypic analysis showed that both fused genes rescued the orange flower phenotype, as all transgenic plants produced yellow flowers (Fig. 2, A to C). Consistent with this result, reverse transcription quantitative PCR (RT-qPCR) analysis of the petals showed that the *BnaA09.ZEPpro:BnaA07.ZEP* and *BnaC09.ZEPpro:BnaC07.ZEP* transgenic lines showed dramatic increases in the transcript abundance of *BnaA07.ZEP* and *BnaC07.ZEP*, respectively, compared with O271 (Fig. 2, D and E). These results indicate that these 2 pairs of *BnaZEPs* encode proteins with common functions in carotenoid biosynthesis and that variation in their promoter sequences mainly determines their tissue-specific functional divergence.

To identify core regulatory regions in the *BnaZEP* promoters, we placed the *GUS* reporter gene under the control of serial 5′ promoter truncations for the flower-specific genes *Bna.A09.ZEP/Bna.C09.ZEP* and the leaf-specific genes *Bna.A07.ZEP/Bna.C07.ZEP* (Fig. 2, F to I) and then transformed each construct into Arabidopsis. For each *BnaZEP*, we tested 3 promoter fragments. The shortest promoter fragments consisting of only ~100 bp did not drive *GUS* expression in any of the tissues. By contrast, the 2 other promoter fragments succeeded in driving *GUS* expression in leaves or flowers, indicating that these longer promoter fragments contain key cis-elements for the expression of *BnaA09.ZEP*, *BnaC09.ZEP*, *BnaA07.ZEP*, and *BnaC07.ZEP*. We designated the necessary regions present in the *BnaZEP* promoters as core regions hereafter. Using the PlantCARE database (Lescot et al. 2002), we predicted that the core regions of the 4 *BnaZEP* promoters contain the same motifs, including ABRE, WRE3, CAAT-box,
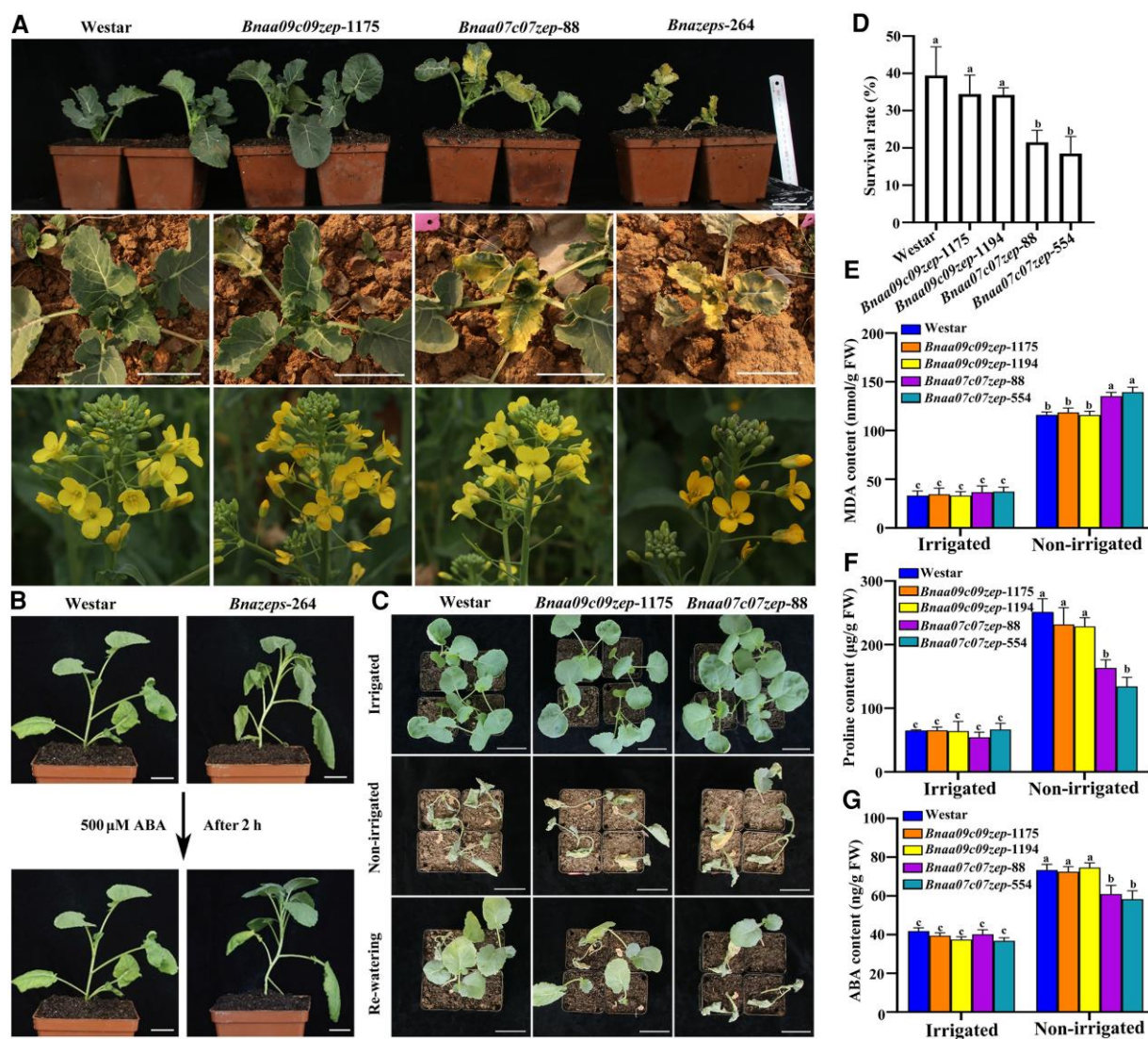
Figure 1. Representative photographs of *BnaZEP* mutants. **A)** Phenotypes of *B. napus* var. Westar (wild type), double mutant lines (*Bnaa09c09zep* and *Bnaa07c07zep*), and quadruple mutant lines (*Bnazeps*) at the seedling stage (first 2 rows) and the flowering stage (third row) in the field. Scale bars, 5 cm. **B)** Effect of ABA treatment on Westar and a quadruple mutant line (*Bnazep*) in the greenhouse. Scale bar, 2 cm. **C)** Phenotypes of Westar and double mutant lines (*Bnaa09c09zep* and *Bnaa07c07zep*) under drought stress. Scale bar, 5 cm. **D)** Survival rates of Westar, *Bnaa09c09zep*, and *Bnaa07c07zep* after rewatering. Sample size is >30, with 3 biological replicates. Contents of MDA **E)**, proline **F)**, and ABA **G)** in Westar, *Bnaa09c09zep*, and *Bnaa07c07zep* plants before and after drought stress. Every sample was collected from 5 individuals, with 3 biological replicates (for a total of 15 individuals). Data represent the mean ± SD from 3 biological replicates. Different lowercase letters indicate significant differences by ANOVA followed by Tukey's post hoc test in the SPSS program ($P < 0.05$). The defined error bars and statistical analyses apply to all bar graphs in this figure.

and CGTCA-motifs (Supplementary Fig. S5). Remarkably, MYC and ARE motifs were specific to the core regions of *BnaA07.ZEP*/*BnaC07.ZEP* promoters, whereas MYB recognition motifs were present particularly in the *BnaA09.ZEP*/*BnaC09.ZEP* promoters. These analyses suggest that shared and distinct transcriptional regulators control the expression of the 2 pairs of *BnaZEPs*.

BnaABF3s are shared regulators that bind to the promoters of all 4 *BnaZEPs*

A yeast 1-hybrid (Y1H) screen was performed to identify the TFs that bind to the *BnaZEP* promoters. Since the core regions of

BnaA09.ZEP and *BnaC09.ZEP* promoters drove the expression of the reporter gene in yeast, precluding their direct use, we used the core region of the *BnaC07.ZEP* promoter as bait. Among the several TFs we obtained, one was a bZIP TF BnaC07.ABF3, a homolog of ABF3 in Arabidopsis. Using the protein sequence of AtABF3 as a query, we identified 2 more copies of *BnaC07.ABF3* in the *B. napus* genome, namely, *BnaC01.ABF3* and *BnaA01.ABF3* (Supplementary Fig. S6). The 3 BnaABFs contain a highly conserved bZIP domain that resembles that of AtABF3 (Supplementary Fig. S7) in their N-terminal regions.

As shown in Fig. 3A and Supplementary Fig. S5, the core regions of each *BnaZEP* promoter contain 2 ABREs (ABRE1
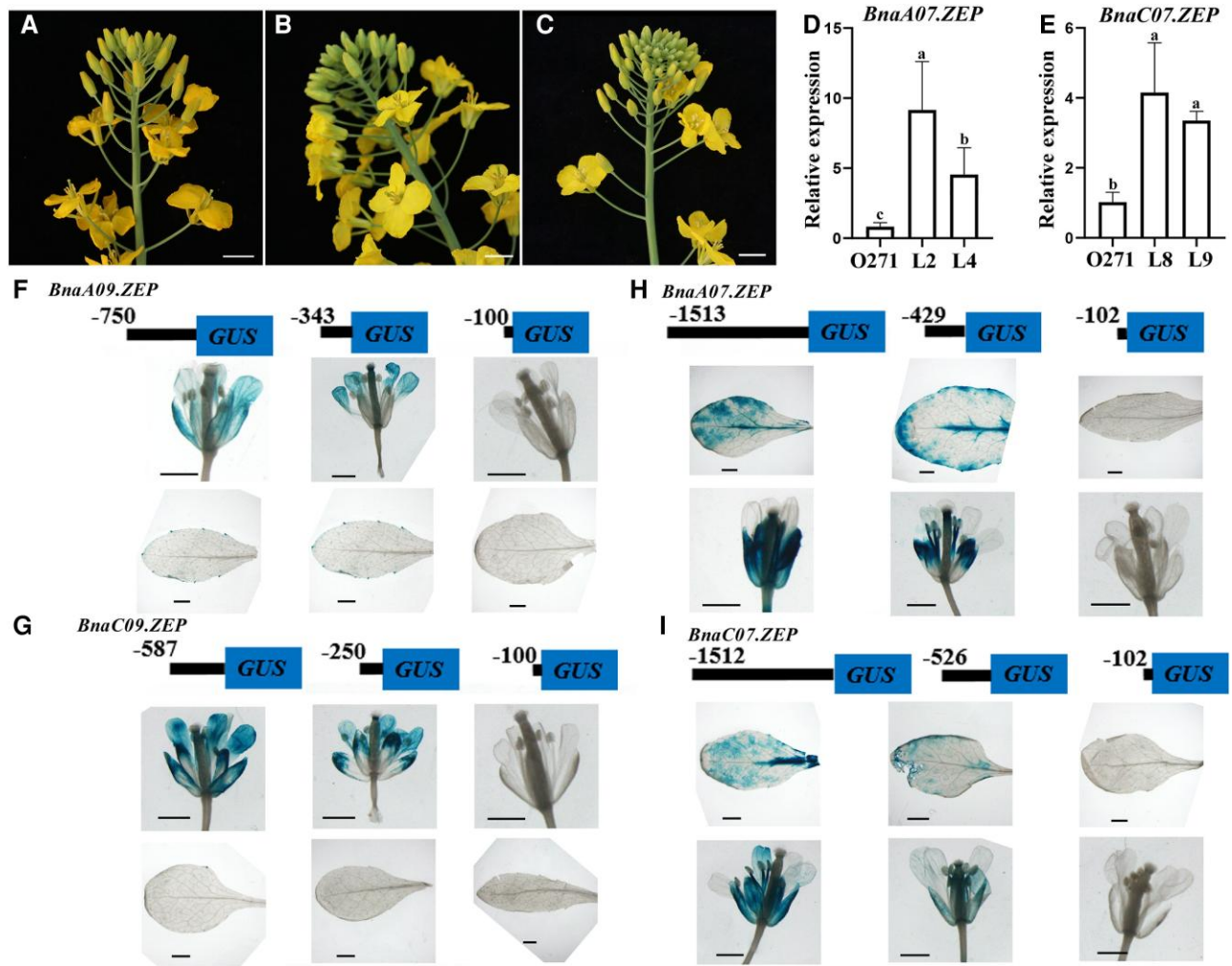
Figure 2. The functional divergence of *BnaZEP*s is mainly determined by their promoters. Inflorescence of O271 **A**), a *BnaA09.ZEPpro:BnaA07.ZEP* transgenic line **B**), and a *BnaC09.ZEPpro:BnaC07.ZEP* transgenic line **C**). Scale bars, 1 cm. Relative expression levels of *BnaA07.ZEP* **D**) and *BnaC07.ZEP* **E**) in 4- to 5-mm petals from the flowers of *BnaA09.ZEPpro:BnaA07.ZEP* (L2, L4) and *BnaC09.ZEPpro:BnaC07.ZEP* (L8, L9) transgenic lines. Data represent the mean ± SD from 3 biological replicates. Different lowercase letters indicate significant differences by ANOVA followed by Tukey's test (*P* < 0.05). Representative GUS staining derived from the promoter fragments of *BnaA09.ZEP* **F**), *BnaC09.ZEP* **G**), *BnaA07.ZEP* **H**), or *BnaC07.ZEP* **I**) used to drive the expression of the *GUS* reporter gene in transgenic Arabidopsis plants containing the indicated promoter fragment. Scale bars of leaves, 2 mm; Scale bars of petals, 1 mm.

and ABRE2), which are putative binding motifs of bZIP TFs (Uno et al. 2000). Considering that each pair of *BnaZEP*s has nearly identical sequences flanking their ABRE1 and ABRE2 motifs (Fig. 3A), we conducted a Y1H assay using the *BnaC07.ZEP* and *BnaA09.ZEP* promoters to test whether BnaABF3s directly bind to either or both ABREs. Accordingly, *BnaC07.ZEP* promoter fragments C07-1 and C07-2, which contain ABRE1 and ABRE2, respectively (Fig. 3A), were used as bait. Compared with the negative control, the presence of C07-1 and *BnaABF3*s allowed yeast cells to survive on dropout medium with 200 ng/mL Aureobasidin A (AbA; Fig. 3B). However, yeast cells carrying the C07-2 fragment cloned into the pAbAi vector and expressing *BnaABF3*s did not grow, demonstrating that BnaABF3s bind to ABRE1 but not to ABRE2 in yeast.

We repeated the assay using the A09-1 fragment, containing ABRE1 from the *BnaA09.ZEP* promoter and cloned into the pAbAi vector (Fig. 3A). Compared with the negative control, yeast cells carrying the A09-1 fragment cloned into pAbAi, and expressing *BnaABF3*s were able to grow on synthetic defined (SD) medium containing 500 ng/mL AbA (Fig. 3B). These results indicate that BnaABF3s bind to ABRE1 in the promoters of all *BnaZEP*s. To obtain independent confirmation of these results, we performed an electrophoretic mobility shift assay (EMSA) using recombinant purified BnaABF3s and the ABRE1 motif present in the *BnaZEP* promoters. We established that His-tagged BnaC07.ABF3, His-BnaC01.ABF3, and His-BnaA01.ABF3 specifically bound to labeled probes corresponding to the C07-1 or A09-1 fragments containing the ABRE1 motif (Fig. 3C). This binding
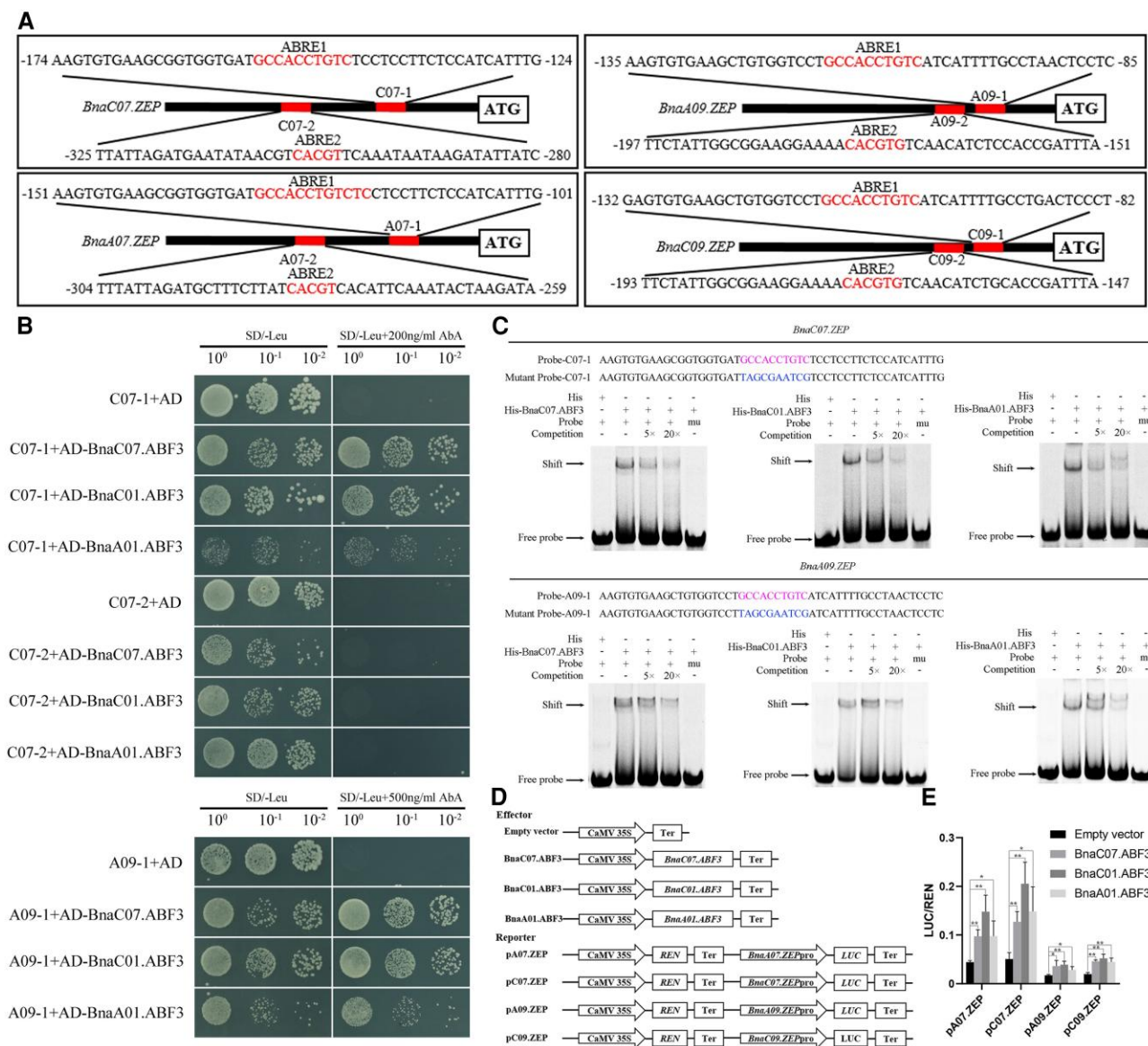
Figure 3. BnaABF3s directly target all 4 *BnaZEP*s. **A)** Diagram of the *BnaZEP* promoters, showing the positions of the ABRE in each core promoter region. C07-1, C07-2, A07-1, A07-2, A09-1, A09-2, C09-1, and C09-2 indicate promoter fragments containing ABREs in the *BnaZEP* promoters. **B)** Y1H assays showing that BnaABF3s bind directly to ABRE1 in the *BnaZEP* promoters but not to ABRE2. Transformed yeast cells were grown on SD medium lacking Leu alone or containing AbA. 10^0, 10^{-1}, and 10^{-2} indicate the dilution of the yeast cultures prior to being spotted onto the plates. C07-1, C07-2, and A09-1 represent the promoter fragments shown in **A)**. AD, pGADT7 vector. **C)** EMSA showing the binding of recombinant BnaABF3s to the *BnaC07.ZEP* and *BnaA09.ZEP* promoters. Five- and 20-fold unlabeled probes were used as cold competitors. "+" and "−" indicate presence and absence, respectively. "mu" represents mutant probe. **D)** Diagrams of the reporter and effector constructs used for the dual-LUC transient expression assay. Ter, terminator. **E)** LUC assay showing the transcriptional activation of the *BnaZEP* promoters by BnaABF3s. The LUC/REN ratio reflects transactivation activity. Data represent the mean ± SD from 3 biological replicates. The asterisks indicate significant differences by Student's *t*-test: *$P < 0.05$; **$P < 0.01$.

was competed out by the addition of unlabeled competitor probes with the same sequence. By contrast, His-BnaABF3s did not bind to the probes containing a mutated version of ABRE1, indicating that BnaABF3s may directly bind to the promoters and regulate the expression of *BnaZEP*s. A dual-luciferase (LUC) assay (Fig. 3D) also showed that each of the 3 BnaABF3s activates the expression of the LUC reporter driven by each *BnaZEP* promoter (Fig. 3E). Overall, these findings

suggest that BnaABF3s directly activate the expression of *BnaZEP*s. Additionally, our LUC, EMSA (Supplementary Fig. S8, A to D), and reanalysis (Supplementary Fig. S8E) of a previous chromatin immunoprecipitation sequencing (ChIP-seq) dataset in Arabidopsis (Song et al. 2016) showed that AtABF3 can directly bind to the *AtZEP* promoter, indicating that the interaction between ABF3 and ZEP is conserved in Arabidopsis.

Characterization of BnaABF3s and their roles in the carotenoid and ABA pathways

An examination of the BnIR database (http://yanglab.hzau.edu.cn/) revealed that *BnaABF3*s are constitutively expressed, with the highest expression seen for *BnaA01.ABF3* and *BnaC07.ABF3* in flower organs, whereas *BnaA01.ABF3* and *BnaC01.ABF3* were most highly expressed in leaves and roots (Supplementary Fig. S9A). Subcellular localization analysis showed that BnaABF3s are nuclear proteins (Supplementary Fig. S9B). Under ABA treatment, the expression levels of *BnaABF3*s were quickly and significantly upregulated (Supplementary Fig. S9C), suggesting that *BnaABF3*s are ABA-inducible TFs.

To investigate the role of *BnaABF3*s in regulating *BnaZEP* expression, we generated transgenic lines in the Westar background overexpressing *BnaC07.ABF3*, *BnaC01.ABF3*, or *BnaA01.ABF3* individually under the control of the cauliflower mosaic virus (CaMV) 35S promoter. For each gene, we used 2 overexpression lines (OE-*BnaABF3*) for subsequent analysis (Supplementary Fig. S10). RT-qPCR analysis showed that *BnaZEP*s transcript levels in these OE-*BnaABF3* lines were 2 to 3 times higher than in Westar (Fig. 4A). However, the phenotype and ABA content of OE-*BnaABF3* were not distinguishable from those of Westar under well-watered conditions (Fig. 4, B to D). Under drought stress, all OE-*BnaABF3* lines showed significantly higher survival rates (36.2% to 40.4%) than Westar (5.0% on average; Fig. 4, B and C). In agreement with this result, the MDA and proline contents of OE-*BnaABF3* plants were significantly lower and higher than in Westar, respectively (Fig. 4, E and F). Moreover, the ABA content of OE-*BnaABF3* was 12.9% to 26.1% higher than that of Westar after exposure to drought stress (Fig. 4D). Together, these results suggest that the 3 BnaABF3 members redundantly activate the transcription of *BnaZEP*s and positively regulate ABA accumulation under drought stress.

To further determine the function of BnaABF3s, we generated a triple mutant by simultaneously knocking out the 3 *BnaABF3* duplicates via CRISPR/Cas9 (Supplementary Fig. S11, A and B). In these lines, all the target alleles were null and exhibited premature translation termination. Under normal growth conditions, the phenotype of *Bnaabf3*s appeared similar to that of Westar (Supplementary Fig. S11C), with no significant difference in the ABA content of leaves and petals from *Bnaabf3*s and Westar (Supplementary Fig. S11D). However, *Bnaabf3*s exhibited a slightly decreased tolerance to simulated drought and weighed significantly less than wild-type seedlings under PEG treatment (Supplementary Fig. S11, E and F).

To understand the consequences of the dysfunction of BnaABF3s, we performed RNA-seq analysis in *Bnaabf3*s and Westar (Supplementary Table S1 and Fig. S12). We identified 6,508 and 2,156 differentially expressed genes (DEGs) in leaves and petals, respectively. Most carotenoid biosynthetic genes, including *BnaA09.ZEP* and *BnaC09.ZEP*, were slightly but not significantly downregulated in the leaves and petals

of *Bnaabf3*s (Supplementary Fig. S12B). Only one gene, *BnaC04.PDS*, was significantly and greatly downregulated 624-fold in *Bnaabf3* leaves. In petals, the loss of *BnaABF3*s significantly altered the expression of 4 genes, upregulating the expression of *BnaC03.PSY* and *BnaC03.LCYB* and downregulating the expression of *BnaC04.PDS* and *BnaA03.BCH1*. lipoxygenases (*BnaA08.LOX3* and *BnaC02.LOX4*), which encode putative lipoxygenases that promote carotenoid degradation through co-oxidation (Gayen et al. 2015), were the only 2 genes from the carotenoid degradation pathway showing significant upregulation in the leaves of the mutant. Although their transcript levels were significantly higher in *Bnaabf3*s than in Westar, their fragments per kilobase of exon model per million mapped reads (FPKM) values (<2) in *Bnaabf3* were relatively low in leaves. By contrast, *BnaC02.LOX4* was more highly expressed (average FPKM of 43.5) in Westar petals and was the only gene related to carotenoid degradation with a significant downregulation in *Bnaabf3*s, suggesting that *BnaC02.LOX4* has a key role in carotenoid homeostasis in petals but not in leaves. We conducted a similar analysis of genes involved in ABA biosynthesis and signaling (Supplementary Fig. S12B). In the ABA biosynthesis pathway, one respective gene showed significantly different expression between Westar and *Bnaabf3*s in each tissue. In terms of the ABA signaling pathway, we detected 4 and 2 genes as being differentially regulated in leaves and petals, respectively. Among them, *BnaC06.ABF1*, a homologous gene of *BnaABF3*s, was significantly upregulated in leaves, suggesting that *BnaC06.ABF1* may become more highly expressed in *Bnaabf3* for functional compensation and ensuring a relatively stable ABA content in leaves in response to *BnaABF3*s mutation. Taken together, these results suggest that BnaABF3s are involved in partially similar but different regulatory networks for carotenoid and ABA metabolism in leaves and flowers.

BnaMYB44s are negative regulators specifically targeting the BnaA09.ZEP and BnaC09.ZEP promoters

As an R2R3-MYB TF, AtMYB44 plays an important role in ABA-induced responses and regulates gene expression by binding to a specific DNA sequence, 5′-TAACTG-3′, in the promoters of its target genes (Jung et al. 2008; Liu et al. 2011). Sequence analysis revealed that this specific sequence is present in the *BnaA09.ZEP*/*BnaC09.ZEP* promoters, but not in the *BnaA07.ZEP*/*BnaC07.ZEP* promoters (Fig. 5A and Supplementary Fig. S5), raising the possibility that BnaMYB44s specifically bind to the *BnaA09.ZEP*/*BnaC09.ZEP* promoters. Using the AtMYB44 sequence as the query in a BLAST search of the *B. napus* database, we identified BnaC07.MYB44 and BnaA07.MYB44 as 2 putative MYB44 homologs (Supplementary Fig. S13). *BnaC07.MYB44* and *BnaA07.MYB44* showed expression patterns similar to those of *BnaA09.ZEP* and *BnaC09.ZEP*, with high transcript levels in flower organs (Supplementary Fig. S14, A and B). Furthermore, BnaMYB44s localized to the nucleus of *Nicotiana benthamiana*, as might
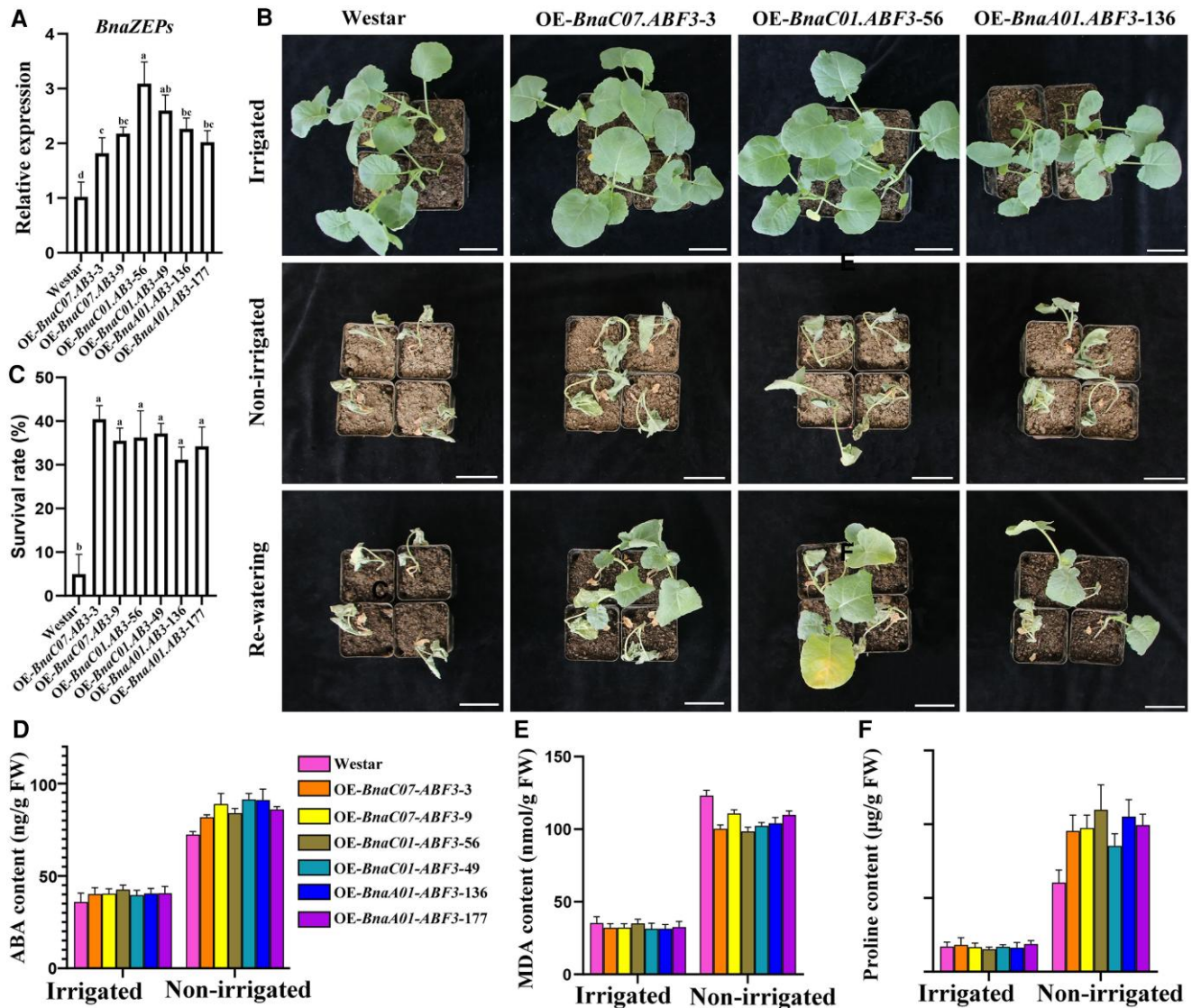
Figure 4. Performance of *BnaABF3*-overexpressing lines under drought stress. **A)** Expression levels of *BnaZEPs* in OE-*BnaC07.ABF3*, OE-*BnaC01.ABF3*, and OE-*BnaA01.ABF3* leaves. Each tissue sample was collected from 3 plants per biological replicate, with 3 biological replicates. **B)** Images showing the phenotypes of *B. napus* var. Westar (wild type), OE-*BnaC07.ABF3*, OE-*BnaC01.ABF3*, and OE-*BnaA01.ABF3* under drought stress. Scale bars, 5 cm. OE, overexpression. **C)** Survival rates of Westar and *BnaABF3*-overexpressing lines after rewatering. Sample size is >30, with 3 biological replicates. Content of ABA **D)**, MDA **E)**, and proline **F)** in Westar and *BnaABF3*-overexpressing lines before and after drought stress. Every sample was collected from 5 individuals, with 3 biological replicates (a total of 15 individuals). Data represent the mean $\pm$ SD from 3 biological replicates. Different lowercase letters indicate significant differences by ANOVA followed by Tukey's post hoc test in the SPSS program ($P < 0.05$). The defined error bars and statistical analyses apply to all bar graphs in this figure.

be expected for a TF that binds to the promoter of its target genes (Supplementary Fig. S14C). An EMSA showed that recombinant purified BnaC07.MYB44 and BnaA07.MYB44 both bound to a labeled probe (probe-C09-MYB) containing the MYB-binding site (Fig. 5B). The intensity of the shifted band declined with the addition of greater amounts of unlabeled intact probe, while neither recombinant protein bound to a labeled probe with a mutated MYB motif. A dual-LUC assay further supported the idea that BnaMYB44s can bind to the promoters of *BnaA09.ZEP* and *BnaC09.ZEP* and repress their transcriptional outputs (Fig. 5, C and D). These results suggest that BnaC07.MYB44 and BnaA07.MYB44 specifically target the *BnaA09.ZEP* and *BnaC09.ZEP* promoters as transcriptional repressors.

Overexpression of *BnaA07.MYB44* influences plant hormone signaling, phenylpropanoid, and carotenoid pathways in *B. napus* petals

To explore the function of BnaMYB44 in *B. napus*, we generated *BnaA07.MYB44*-overexpressing transgenic lines (OE-*BnaA07.MYB44*). RT-qPCR analysis showed that the
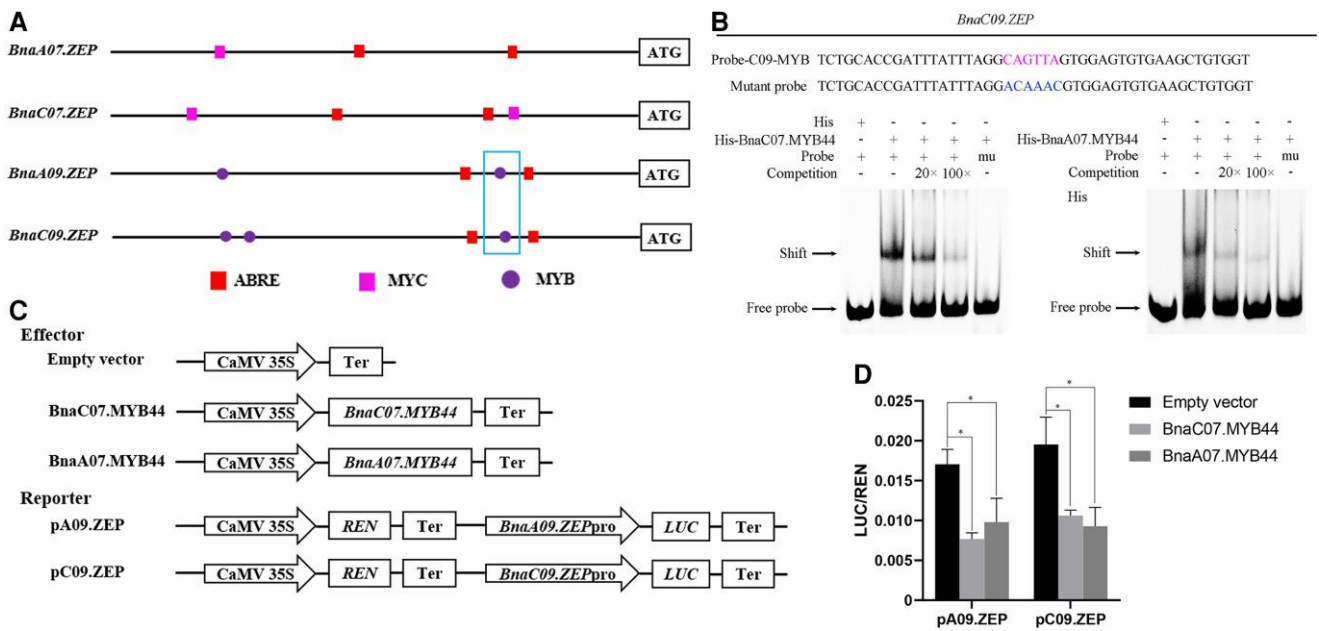
Figure 5. BnaC07.MYB44 and BnaA07.MYB44 specifically target the *BnaA09.ZEP* and *BnaC09.ZEP* promoters. **A)** Diagram of the *BnaZEP* promoters showing the putative cis-elements in the 500-bp region upstream of the ATG. The specific MYB motif (5′-TAACTG-3′) is framed in blue. **B)** EMSA showing the binding of recombinant BnaC07.MYB44 and BnaA07.MYB44 to the *BnaC09.ZEP* promoter. Twenty- and 100-fold unlabeled probes were used as competitors. "+" and "−" indicate presence and absence, respectively. "mu" represents mutant probe. **C)** Diagrams of the reporter and effector constructs used for the dual-LUC transient expression assay. Ter, terminator. **D)** LUC assay showing the activation of the *BnaA09.ZEP* and *BnaC09.ZEP* promoters by BnaC07.MYB44 and BnaA07.MYB44. The LUC/REN ratio reflects transactivation activity. Data represent the means ± SD from 3 biological replicates. Asterisks indicate significant differences by Student's *t*-test; *$P < 0.05$.

transcript levels of *BnaA09.ZEP* and *BnaC09.ZEP* in OE-*BnaA07. MYB44* were significantly lower (38.9% and 44.8%, respectively) compared with the control (Fig. 6A). However, the overall phenotype of OE-*BnaA07.MYB44* was comparable with that of Westar, with yellow flowers (Fig. 6B). To determine the effect of *BnaA07.MYB44* on carotenoid biosynthesis, we analyzed the carotenoid profiles of OE-*BnaA07.MYB44* and Westar petals (Fig. 6C). The results showed that the petals from OE-*BnaA07.MYB44* contain significantly more carotenoids (284.15 ± 3.78 µg/g) than Westar (248.24 ± 8.72 µg/g). Lutein is the most abundant carotenoid, accounting for 59.1% to 62.9% of the total carotenoid content in all samples. Overexpressing *BnaA07.MYB44* led to a significant accumulation of lutein in petals, with levels being 17.7% higher in OE-BnaA07.MYB44 than in Westar. These data indicate that BnaA07.MYB44 fine-tunes flower carotenoid accumulation via inhibition of *BnaA09.ZEP* and *BnaC09.ZEP* transcription.

To investigate the regulatory role of BnaA07.MYB44 in carotenoid metabolism and other aspects of plant physiology, we performed an RNA-seq analysis of petals from OE-*BnaA07. MYB44* and Westar. A total of 2,728 upregulated and 1,525 downregulated DEGs were identified (Fig. 6D). A Kyoto Encyclopedia of Genes and Genomes (KEGG) pathway enrichment analysis showed that these DEGs were most enriched in plant hormone signal transduction pathways, such as for auxin, cytokinin, jasmonic acid, and ABA (Supplementary Fig. S15, A and B), indicating that *BnaMYB44* is involved in phytohormone

signaling crosstalk. The second most enriched pathway was the phenylpropanoid pathway. Most phenylpropanoid structural genes were significantly downregulated in OE-*BnaA07.MYB44* compared with Westar (Supplementary Fig. S15C), indicating that BnaMYB44 functions as a repressor in phenylpropanoid biosynthesis in *B. napus* flowers. With respect to the carotenoid biosynthesis pathway, *BnaA09.ZEP* and *BnaC09.ZEP* were downregulated 1.7-fold and 1.3-fold, respectively. Only *BnaA10.PSY* was downregulated about 2-fold in OE-*BnaA07.MYB44*; other genes did not show significant changes in their expression levels (Fig. 6E). However, genes involved in carotenoid degradation, such as *BnaC01.CCD4*, *BnaC02.LOX4*, and *9-cis-epoxycarotenoid dioxygenase 9* (*BnaC06.NCED9*), were significantly upregulated (*BnaC01.CCD4*) or downregulated (*BnaC02.LOX4* and *BnaC06. NCED9*) in OE-*BnaA07.MYB44*. Remarkably, *BnaC02.LOX4* was highly expressed in Westar (average FPKM of 43.47) but was expressed at much lower levels in OE-*BnaA07.MYB44*, with a 6.7-fold decrease in its transcript levels, suggesting that BnaA07.MYB44 may promote carotenoid accumulation by repressing carotenoid degradation.

Discussion

Tight control of *BnaZEP* expression by multiple TFs
The *B. napus* genome comprises 4 copies of *BnaZEP*, forming 2 pairs of duplicated genes in this polyploid species, offering a unique opportunity to explore the mechanisms underlying
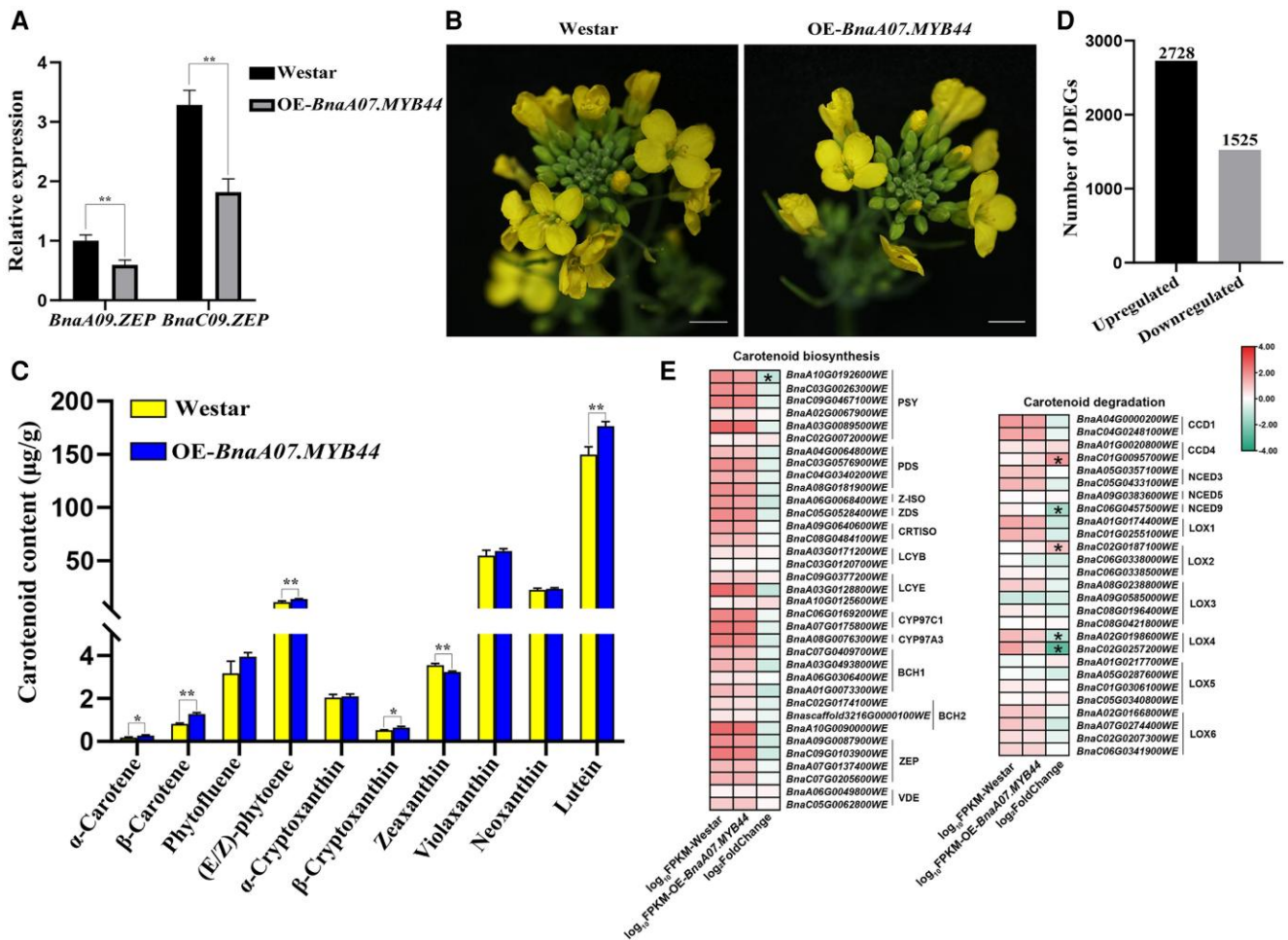
Figure 6. Characterization and RNA-seq analysis of *BnaA07.MYB44*-overexpressing lines. **A)** Relative expression levels of *BnaA09.ZEP* and *BnaC09.ZEP* in Westar and OE-*BnaA07.MYB44* by RT-qPCR analysis. Asterisks indicate significant differences by Student's *t*-test; **$P < 0.01$. Each tissue sample was collected from 3 plants per biological replicate, with 3 biological replicates. Data represent the means ± SD from 3 biological replicates. **B)** Representative photograph of an inflorescence from the control Westar and OE-*BnaA07.MYB44*, showing no flower color difference between them. Scale bars, 1 cm. **C)** The levels of carotenoid components in freshly opened petals of Westar and OE-*BnaA07.MYB44*. Error bars indicate SD from 3 biological replicates. Asterisks indicate significant differences by Student's *t*-test: *$P < 0.05$; **$P < 0.01$. **D)** Number of upregulated and downregulated DEGs in OE-*BnaA07.MYB44* compared to Westar. **E)** Expression differences of genes related to carotenoid biosynthesis and degradation in Westar vs. OE-*BnaA07.MYB44*. The asterisks in the heatmap indicate significant differences between Westar and OE-*BnaA07.MYB44*. The significant differences were defined with a FDR ≤0.05 and an absolute Log_2 (fold-change) ≥1. The red to cyan gradient in the heatmaps indicates Log_2 (fold-change) values from high to low, respectively.

their functional redundancy and diversification. We showed here that the core regions of *BnaZEP* promoters share several cis-elements, such as ABRE, CAAT-box, WRE3, and CGTCA-motifs (Supplementary Fig. S5), indicating that common regulators might be involved in the regulatory network of *BnaZEP*s. In support of this hypothesis, we identified BnaABF3s as direct transcriptional regulators of the 4 *BnaZEP*s in carotenoid and ABA biosynthesis. We also established that BnaMYB44s are transcriptional repressors that differentially regulate the gene pairs *BnaA09.ZEP/BnaC09.ZEP* and *BnaA07.ZEP/BnaC07.ZEP* (Figs. 5B, 5D, and 6A), providing evidence that MYB44 affects carotenoid-related genes at the transcriptional level (He et al. 2022).

We speculate that other regulators may collaboratively modulate the transcription of *BnaZEP*s. In addition to ABRE cis-elements, the promoters of *BnaZEP*s contain 1 WRE3 and 1 to 6 CAAT-box binding sites. Thus, the stress-responsive WRE3 motif and the tissue-specific cis-acting element CAAT-box (Liu et al. 2019a) might also be targets for regulators involved in *BnaZEP* expression. Notably, MYC motifs were exclusively present in the core regions of *BnaA07.ZEP/ BnaC07.ZEP* promoters (Supplementary Fig. S5). This result, together with the fact that the MYC recognition site is usually involved in drought, ABA, and cold signaling (Liu et al. 2019a), suggests that MYC TFs may specifically bind to the *BnaA07.ZEP* and *BnaC07.ZEP* promoters. Additionally, several homologs of *BnaABF3* and *BnaMYB44* in *B. napus* might

participate in the regulation of *BnaZEP* expression. In support of this possibility, *BnaC06.ABF1* expression was significantly enhanced in leaves of *Bnaabf3*s (Supplementary Fig. S12B), whereas the expression of *MYB73* (*BnaC08G0254800WE*) and *MYB77* (*Bnascaffold17160001700WE* and *BnaA08 G0167800WE*) was significantly decreased in OE-*BnaA07. MYB44* petals (Supplementary Fig. S15C). Overall, the combinatorial action of shared and unique regulators is likely to shape the precise regulation of the pairs of *BnaZEP* genes. It would be interesting to identify and verify the function of regulators that specifically target each pair of *BnaZEPs*.

The dual role of BnaABF3s in ABA biosynthesis and signaling pathways

Although the structural genes involved in carotenoid and ABA biosynthesis have been well characterized (Nisar et al. 2015; Chen et al. 2020), the TFs that directly regulate their expression have not. Furthermore, the expression of several carotenoid and ABA biosynthetic genes, such as *PSY2* in carrot (*Daucus carota*), *PSY3* in maize (*Zea mays*), *BCH* in rice (*Oryza sativa*), and *ZEP* in Arabidopsis, was substantially induced by exogenous ABA treatment (Barrero et al. 2006; Li et al. 2008; Du et al. 2010; Simpson et al. 2018). In *B. napus*, the expression of *BnaZEPs* was also upregulated in response to ABA treatment (http://yanglab.hzau.edu.cn/BnIR/eFP_single_gene). However, the mechanism underlying ABA-dependent induction of these genes is still unclear, indicating a missing link of regulators between the ABA signal and its responsive structural genes.

ABFs are bZIP TFs required for ABA-mediated responses that specially bind to the ABRE motif in the promoters of their target genes. ABF3 is a well-known positive regulator of the ABA signaling pathway in Arabidopsis. Overexpressing *ABF3* increased tolerance to drought, salt, cold, and high temperature in several plant species (Kim et al. 2004; Wang et al. 2016; Yang et al. 2020). Further, we showed here that *BnaABF3*s were ABA-inducible and positively regulated ABA biosynthesis and drought tolerance by directly targeting *BnaZEP* promoters and modulating their transcription (Fig. 4B and Supplementary Fig. S11C). The interaction between ABF3 and *ZEP* was also confirmed in Arabidopsis (Supplementary Fig. S8, B to E), indicating that this regulatory relationship is conserved across species. These results highlight a specific function for *ABF3* in carotenoid and ABA biosynthesis and reveal that ABF3 acts as a bridge between the ABA signal and ABA-inducible *ZEP*. A similar dual role of regulators in ABA biosynthesis and signaling was reported by Zong et al. (2016), who found that the ABA signaling factor OsbZIP23 positively regulated the transcription of *OsNCED4* in rice (Zong et al. 2016). Additionally, the *BnaC04.PDS* promoter also contains 3 ABRE elements (Supplementary Fig. S16), and its expression was greatly and significantly downregulated in both leaves and petals of *Bnaabf3*s (Supplementary Fig. S12B), indicating that *BnaC04.PDS* might also be a direct target of BnaABF3s, although further analysis is required.

Possible coordinated regulation of BnaMYB44s in carotenoid, phenylpropanoid, and flavonoid biosynthetic pathways

MYB44 is a member of the R2R3 MYB subgroup 22 TF family in Arabidopsis (Kranz et al. 1998). As a multifaceted TF, MYB44 has been reported to be involved in seed germination (Nguyen et al. 2012), disease resistance (Wang et al. 2023), and drought, heat, and salt tolerance (Jung et al. 2008; Jaradat et al. 2013; Li et al. 2021; Zhang et al. 2022). However, the functional multiplicity of MYB44 was mainly explored in Arabidopsis; thus, further investigations into other species are required, especially regarding its regulation in other tissues such as flowers. In this study, we showed that BnaMYB44s positively fine-tune the accumulation of flower carotenoids by directly targeting and downregulating the transcription of *BnaA09.ZEP* and *BnaC09.ZEP*. RNA-seq analysis also indicated that *BnaA10.PSY* might be a direct target of BnaMYB44 (Fig. 6, A, C, and E). These results are different from a recent study reporting that MYB44 might promote carotenoid biosynthesis by directly binding to the *PDS* promoter in *Ulva prolifera* (He et al. 2022). The discrepancy might be attributed to the differences between plants and algae. Overexpression of *BnaA07.MYB44* did not produce phenotypic differences compared with Westar, as we only observed a 1.7-/1.3-fold decrease in *BnaA09.ZEP/BnaC09.ZEP* transcript levels that was not accompanied by a change in flower color in OE-*BnaA07.MYB44*. This result may reflect a transcriptional auto-regulation within the R2R3 MYB S22 subfamily. Members of the MYB S22 subfamily, including MYB44, MYB70, MYB73, and MYB77, exhibit partially redundant functions in ABA signaling, stress responses, and leaf senescence (Jaradat et al. 2013). In agreement, our RNA-seq analysis showed that *BnaA07.MYB44* overexpression associates with significant downregulation of *BnaMYB73* and *BnaC08. MYB77*. Further evidence supporting the transcriptional auto-regulation within the MYB S22 subfamily came from Arabidopsis, in which *MYB70*, *MYB73*, and *MYB77* were significantly repressed in *MYB44*-overexpressing lines (Persak and Pitzschke 2013). Nevertheless, the indicated transcriptional auto-regulation and cross-regulation among *BnaMYB44*, *BnaMYB73*, and *BnaMYB77* in carotenoid biosynthesis need to be elucidated in *B. napus* in the future.

A growing body of evidence has demonstrated the existence of crosstalk between the carotenoid and flavonoid biosynthetic pathways (Davuluri et al. 2005; Sagawa et al. 2016; Meng et al. 2019; Liu et al. 2020); however, the regulatory nodes that integrate these 2 pathways remain largely unknown. Recently, MYB44 was reported to be a negative regulator of anthocyanin biosynthesis in potato (*Solanum tuberosum*) and tree peony (*Paeonia suffruticosa*; Liu et al. 2019b; Luan et al. 2023). In line with these observations, we showed that the expression of several genes involved in the flavonoid pathway and most genes related to the upstream phenylpropanoid pathway was significantly downregulated when *BnaA07.MYB44* was overexpressed (Supplementary
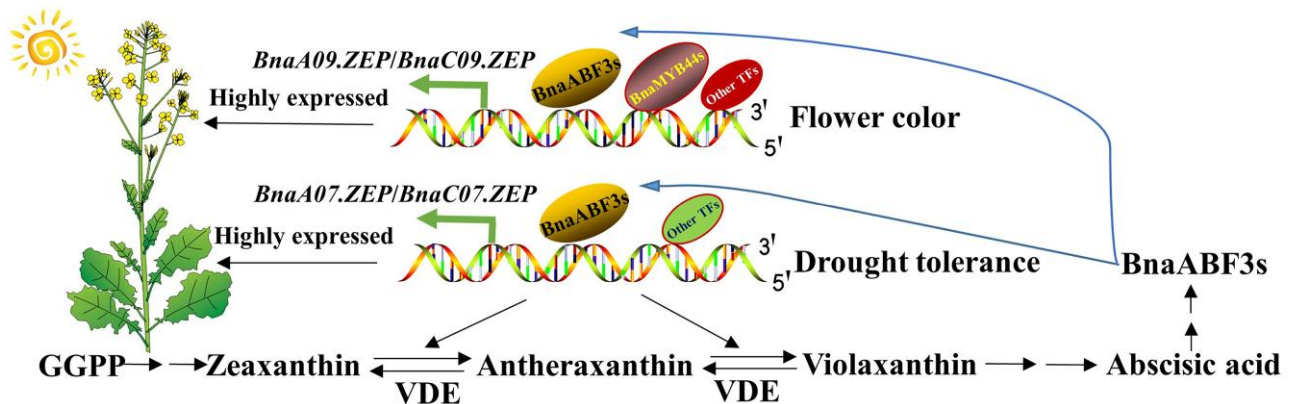
Figure 7. Working model of TF-mediated regulation of *BnaZEP* transcription in *B. napus*. The 4 BnaZEPs form 2 pairs (BnaA09.ZEP/BnaC09.ZEP and BnaA07.ZEP/BnaC07.ZEP), both of which participate in the conversion of zeaxanthin to violaxanthin in petals and leaves, respectively. The ABA signaling factors, BnaABF3s, directly bind to the *BnaZEP* promoters and positively regulate *BnaZEP* expression through a positive feedback mechanism. Due to the variation in the cis-elements between the 2 pairs, different TFs bind to them. For example, BnaMYB44s specifically target the *BnaA09.ZEP* and *BnaC09.ZEP* promoters.

Fig. S15C), indicating that MYB44 represses phenylpropanoid and flavonoid biosynthesis. Thus, BnaMYB44 might be a regulatory component that provides crosstalk between the carotenoid, phenylpropanoid, and flavonoid biosynthetic pathways in *B. napus*.

In conclusion, *BnaZEP*s possess distinct regulatory networks that comprise multiple TFs and are more complex than *AtZEP*. Based on our findings and those of previous studies (Nambara and Marion-Poll 2005; Hauser et al. 2011; Chen et al. 2020), we propose a working model that outlines how TFs regulate *BnaZEP*s in *B. napus* (Fig. 7). *BnaA09.ZEP/BnaC09.ZEP* and *BnaA07.ZEP/BnaC07.ZEP* function in the conversion of zeaxanthin to violaxanthin in flowers and leaves, respectively. The ABA signaling factors, BnaABF3s, directly target and upregulate the transcription of *BnaZEP*s through a positive feedback mechanism. Moreover, there are TFs that exclusively bind to *BnaA09.ZEP/BnaC09.ZEP* or *BnaA07.ZEP/BnaC07.ZEP*. For example, BnaMYB44 specifically targets the *BnaA09.ZEP* and *BnaC09.ZEP* promoters and represses their transcription. Overall, this proposed working model expands our knowledge of the intricate regulation of *BnaZEP*s in *B. napus*.

Materials and methods

Plant materials

"O271" is a rapeseed (*B. napus*) mutant that carries loss-of-function alleles for *BnaA09.ZEP* and *BnaC09.ZEP* and exhibits orange flowers (Liu et al. 2020). Yellow-flowering APSP and CPSP are T_2 complementary lines obtained by independently introducing *BnaA09.ZEP* or *BnaC09.ZEP* into the O271 background (Liu et al. 2020). The orange-flowering *Bnaa09c09zep* mutant is a T_2 knockout line produced by simultaneously mutating *BnaA09.ZEP* and *BnaC09.ZEP* in yellow-flowering *B. napus* var. "Westar" using CRISPR/Cas9-mediated genome editing (Liu et al. 2020). All *B. napus* lines and Arabidopsis (*A.* *thaliana*) (Col-0) were grown in a field or in a greenhouse at 22°C under 16-h-light/8-h-dark conditions.

Plasmid construction and plant transformation

To generate double mutants of *BnaA07.ZEP* and *BnaC07.ZEP*, quadruple mutants of *BnaZEP*s, and triple mutants of *BnaABF3s*, 6 single-guide RNAs (sgRNAs) were designed using CRISPR-P (http://crispr.hzau.edu.cn/cgi-bin/CRISPR2/CRISPR). The S1 and S2 sgRNAs targeted both *BnaA07.ZEP* and *BnaC07.ZEP*; the S3 and S4 sgRNAs targeted all *BnaZEP*s (Supplementary Fig. S2A), and the S5 and S6 sgRNAs targeted all 3 *BnaABF3s* (Supplementary Fig. S11A). The CRISPR/Cas9 vectors were constructed as previously described (Xing et al. 2014). In parallel, 4 plasmids were constructed for overexpression. The full-length CDSs of *BnaC07.ABF3*, *BnaC01.ABF3*, *BnaA01.ABF3*, and *BnaA07.MYB44* were individually cloned into the binary vector pCAMBIA2300 harboring the CaMV 35S promoter. All plasmids were introduced into the *Agrobacterium tumefaciens* strain GV3101 and then transformed into Westar (Dun et al. 2011).

The predicted promoter region of *BnaA09.ZEP* (754 bp) combined with the CDS of *BnaA07.ZEP* and the predicted promoter region of *BnaC09.ZEP* (877 bp) combined with the CDS of *BnaC07.ZEP* were separately cloned into the binary vector pCAMBIA2300 to construct the promoter-swapped plasmids *BnaA09.ZEPpro:BnaA07.ZEP* and *BnaC09.ZEPpro:BnaC07.ZEP*, respectively. The resulting plasmids were introduced into the *Agrobacterium* strain GV3101 and transformed into O271. All primers used in this study are listed in Supplementary Table S2.

ABA and drought treatments

To rescue the wilting phenotype of the *Bnazep* mutants, 500-μM ABA was sprayed on leaves every 2 to 3 d when *Bnazep* plants showed signs of wilting. To study the influence of exogenous ABA treatment on *BnaABF3* expression,

4-wk-old Westar seedlings were transferred to Hoagland nutrient solution (Hoagland and Arnon 1950) containing 200 μM ABA. The leaves were collected 0, 2, 4, 6, 12, 24, and 48 h after ABA treatment and stored at −80°C for RT-qPCR analysis. For drought stress assays, transgenic lines and their control plants were grown in pots with a 3:1 volume ratio of soil to vermiculite. All pots were placed in a container and irrigated with water until saturation before treatment. The water in the containers was then allowed to drain. Water withholding treatment was initiated on 4-wk-old seedlings and lasted for 2 or 3 wk, after which irrigation was resumed for 2 d; the survival rate was then scored. Sample size is >30, with 3 biological replicates. For PEG6000 treatment, Westar and *Bnaabf3* seeds were germinated in a nutrient solution with no PEG or 20% (w/v) PEG. After 10 d, the seedlings were collected for photographs, determination of fresh weight, and RT-qPCR analysis.

Measurement of MDA, proline, ABA, and carotenoid content

The leaves of Westar, *Bnaa09c09zep*, *Bnaa07c07zep*, OE-*BnaABF3*, and *Bnaabf3* plants were collected before and after exposure to drought stress and stored at −80°C for measurement of proline, MDA, and ABA content. MDA and proline contents were measured using the respective assay kits (AKFA013M and AKAM003M, BOXBIO, China). ABA profiling was conducted following a previously described method (Yang et al. 2001). Freshly opened petals from O271, APSP, CPSP, Westar, and OE-*BnaA07.MYB44* were collected for carotenoid profiling as previously described (Ye et al. 2022). Every sample consisted of 5 individuals, with 3 biological replicates (for a total of 15 individuals). Data were analyzed by ANOVA and Tukey's test using SPSS V19.0 (IBM, USA).

Observations of leaf stomata by fluorescence microscopy

The lower epidermis of the youngest fully developed leaf was collected from 4-wk-old Westar and *Bnazep* plants. The stomata on the epidermis were imaged using a fluorescence microscope (OLYMPUS, SP8; Leica, Wetzlar, Germany). Three individual plants per genotype were used. Stomatal length and aperture were measured using ImageJ software.

Subcellular localization

The CDSs of *BnaA09.ZEP*, *BnaC09.ZEP*, *BnaA07.ZEP*, and *BnaC07.ZEP* were individually cloned into the pM999 vector to generate proteins fused with GFP. The resulting plasmid was transformed into Arabidopsis protoplast. The CDSs of *BnaC07.ABF3*, *BnaC01.ABF3*, *BnaA01.ABF3*, *BnaA07.MYB44*, and *BnaC07.MYB44* were individually cloned into the pMDC83 vector to generate proteins fused with GFP. The H2B-mCherry protein was used as the nuclear marker for TFs. The resulting plasmid was transformed into *N. benthamiana*. Arabidopsis protoplast isolation, plasmid

transfection, and transient transfection of *N. benthamiana* were performed as described previously (Yoo et al. 2007; Ye et al. 2022). The subcellular localization was captured using a confocal laser scanning confocal microscope (Leica, Wetzlar, Germany). The following lines of an argon ion laser were used: 488 nm for GFP and chlorophyll, 552 nm for mCherry, and emission at 505 to 550 nm for GFP, 600 to 640 nm for mCherry, 636 to 750 nm for chlorophyll.

RNA extraction and RT-qPCR analysis

Total RNA was extracted using an RNA Prep Pure Plant Kit (TIANGEN, DP432, China). Each tissue sample was collected from 3 plants per biological replicate, with 3 biological replicates. RT-qPCR was performed as previously described (Ye et al. 2022), using *BnaActin7* as an internal reference.

Construction of *GUS* reporter plasmids and GUS staining

The truncated promoter fragments of *BnaA09.ZEP*, *BnaC09.ZEP*, *BnaA07.ZEP*, and *BnaC07.ZEP* were individually amplified and cloned into the pCAMBIA2300:GUS vector before being introduced into *Agrobacterium* strain GV3101. Flowering Arabidopsis plants were infiltrated with GV3101 cells using the floral dip method (Clough and Bent 1998). For GUS staining, homozygous T_3 transgenic plants with a single T-DNA insertion were incubated in X-Gluc solution (Biosharp, BL622A, China) at 37°C overnight and subsequently cleared from chlorophylls in 70% (v/v) ethanol, as previously described (Jefferson et al. 1987). The stained tissues were imaged using a stereomicroscope (Olympus Corporation, Shinjuku, Japan).

Y1H assay

For Y1H screening, a cDNA expression library derived from 0.5- to 7-mm buds of *B. napus* and cloned in the pGADT7 vector was used as prey. The 424-bp core region of the *BnaC07.ZEP* promoter (Supplementary Fig. S5) was amplified and cloned into the pAbAi vector to produce the bait plasmid. The resulting plasmid was linearized and transformed into a yeast strain, Y1HGold, to obtain a bait-specific reporter strain. The Y1H screen was performed using the Matchmaker Gold Yeast One-Hybrid Library Screening System (Clontech, 630491, Japan) following the manufacturer's instructions.

For targeted Y1H validation assays, *BnaC07.ZEP* promoter fragments spanning the ABRE1 motif (C07-1: 5′-AAGTG TGAAGCGGTGGTGATGCCACCTGTCTCCTCCTTCTCCAT- CATTTG-3′) and ABRE2 motif (C07-2: 5′-TTATTAGATGAA TATAACGTCACGTTCAAATAATAAGATATTATC-3′), and a *BnaA09.ZEP* promoter fragment spanning the ABRE1 motif (A09-1: 5′- AAGTGTGAAGCTGTGGTCCTGCCACCTGTCAT CATTTTGCCTAACTCCTC-3′) were individually cloned into the pAbAi vector to produce the bait plasmids. The CDSs of *BnaC07.ABF3*, *BnaC01.ABF3*, and *BnaA01.ABF3* were individually cloned into the pGADT7 vector to produce the prey plasmids. The resulting plasmids were transformed

into Y1HGold, harboring the respective bait plasmid (pAbAi-bait); positive transformants were selected on SD medium lacking Leu but containing AbA.

EMSA

The CDSs of *BnaC07.ABF3*, *BnaC01.ABF3*, *BnaA01.ABF3*, *BnaA07.MYB44*, *BnaC07.MYB44*, and *AtABF3* were individually cloned into the pET32a vector to generate fusion proteins with a 6×His tag. The recombinant proteins were expressed in *Escherichia coli* Rosetta (DE3) and then purified using a Ni-NTA 6FF Sefinose (TM) Resin Kit (BBI, C600332, China) following the manufacturer's instructions. Two DNA fragments from the *BnaC07.ZEP* (C07-1) and *BnaA09.ZEP* (A09-1) promoters containing the ABRE1 motif, one DNA fragment from the *BnaC09.ZEP* promoter containing the MYB-binding motif (C09-MYB: 5′-TCTGCACCGATTTATTT AGGCAGTTAGTGGAGTGTGAAGCTGTGGT-3′), and one DNA fragment from the *AtZEP* promoter containing the ABRE1 motif (pAtZEP-ABRE1: 5′-AAGTGTGTTGCGTTGCT GATGCCACCTGTCTCCTCCTCCATCATTTG-3′) were synthesized as Cy5-labeled oligonucleotides. The ABRE motifs in the C07-1 and A09-1 probes were also mutated to "TAGCGAATCG" to generate mutant competitive probes. In addition, the MYB motif in the C09-MYB probe was mutated to "ACAAAC" in the mutant probe; all mutant probes were labeled with Cy5 LUC. Recombinant proteins were incubated with each labeled probe at 25 °C for 20 min. Unlabeled nonmutant probes were used as competitors to examine binding specificity. EMSA was performed using an EMSA/Gel-Shift Kit (Beyotime, GS002, China) following the manufacturer's protocol. Gel images were captured using a Fujifilm FLA-9000 imager (FujiFilm, Tokyo, Japan).

LUC transient expression assay

LUC assays were performed using Arabidopsis mesophyll protoplasts as previously described (Hellens et al. 2005). The CDSs of *BnaC07.ABF3*, *BnaC01.ABF3*, *BnaA01.ABF3*, *BnaA07.MYB44*, *BnaC07.MYB44*, and *AtABF3* were individually cloned into the pGreenII 62-SK vector to generate effector constructs. The promoter fragments of *BnaA09.ZEP*, *BnaC09.ZEP*, *BnaA07.ZEP*, *BnaC07.ZEP*, and *AtZEP* were individually cloned into the pGreenII 0800-LUC vector to generate the reporter constructs. LUC activity was measured using a Dual-Luciferase Reporter Assay System (Promega, E1910, USA). The data are represented as the ratio of LUC values to Renilla LUC (REN) values. Each sample was analyzed in 3 biological replicates.

Sequence alignment and phylogenetic analysis

Amino acid sequences of ABF homologs were obtained from the NCBI website (https://www.ncbi.nlm.nih.gov). Sequences were aligned using MEGA version 7.0 (Kumar et al. 2016) with ClustalW and visualized using GeneDoc as previously described (Ye et al. 2022). The phylogenetic tree was reconstructed with MEGA version 7.0 using the neighbor-joining statistical method with 1,000 bootstrap replications.

ChIP-seq analysis

The ChIP-seq data were downloaded from the NCBI database (GSE80568; Song et al. 2016) and analyzed as previously described (Landt et al. 2012).

RNA-seq analysis

The petals from 5-mm buds were collected from Westar, OE-*BnaA07.MYB44*, and *Bnaabf3* plants. The leaves were collected from 4-wk-old Westar and *Bnaabf3* plants. Each sample consisted of 5 individuals, with 3 biological replicates per genotype (for a total of 15 individuals per genotype). DEGs were defined with a false discovery rate (FDR) ≤0.05 and an absolute Log_2 (fold-change) ≥1 between Westar and the other genotypes. RNA sequencing, data analysis, DEG identification, and KEGG analysis were performed as described previously (Ye et al. 2022).

Accession numbers

Sequence data from this article can be found in the NCBI database or the *Brassicaceae* database (http://brassicadb.cn/#/) under accession numbers *BnaA07.ZEP* (MN057938), *BnaC07.ZEP* (MN057939), *BnaA09.ZEP* (MN057940), *BnaC09.ZEP* (MN057 941), *BnaC07.ABF3* (BnaC07g44670D), *BnaC01.ABF3* (BnaC01g 04330D), *BnaA01.ABF3* (OP643677), *BnaC07.MYB44* (BnaC07g 16030D), *BnaA07.MYB44* (BnaA07g11930D), and *BnaActin7* (BnaC02g00690D). The raw data for the RNA-seq were deposited in the NCBI database under the accession number PRJNA970732.

Author contributions

J.W. designed this study. S.Y. and Y.H. performed most of the experiments. T.M. performed the plant transformations. X.M. performed the sequence alignment and phylogenetic analysis. R.L. performed the ChIP-seq data analysis. J.S. conducted the GUS assay. S.Y. and J.W. wrote the manuscript.

Supplementary data

The following materials are available in the online version of this article.

Supplementary Figure S1. The proteins encoded by the 4 *BnaZEP* genes have similar functions and subcellular localization.

Supplementary Figure S2. *BnaZEP* mutants generated by CRISPR/Cas9 technology.

Supplementary Figure S3. Phenotypes of *Bnazep* mutants.

Supplementary Figure S4. Sequence alignment of the *BnaZEP* promoters (2,000 bp upstream of the start codon).

Supplementary Figure S5. Putative cis-elements in the core regions of the 4 *BnaZEP* promoters using the PlantCARE database (http://bioinformatics.psb.ugent.be/webtools/plantcare/html/).

Supplementary Figure S6. Phylogenetic analysis of ABFs in *B. napus* and closely related species.

Supplementary Figure S7. Amino acid sequence alignment of ABF3 from Arabidopsis and *B. napus*.

Supplementary Figure S8. AtABF3 directly regulates *AtZEP* expression in Arabidopsis.

Supplementary Figure S9. Characterization of *BnaABF3*s in *B. napus*.

Supplementary Figure S10. Relative expression levels of *BnaABF*s in Westar and the *ABF3*-overexpressing lines.

Supplementary Figure S11. Generation and performance of *Bnaabf3* mutants after PEG treatment.

Supplementary Figure S12. Analysis of DEGs identified in the leaves and petals between Westar and *Bnaabf3*s.

Supplementary Figure S13. Amino acid sequence alignment of MYB44 from Arabidopsis and *B. napus*.

Supplementary Figure S14. Characterization of BnaMYB44s in *B. napus*.

Supplementary Figure S15. Analysis of DEGs identified between the petals of Westar and OE-*BnaA07.MYB44*.

Supplementary Figure S16. Diagram of *BnaPDS* promoters showing the position of their ABREs. Each diagram shows the region 2,000-bp upstream of the start codon.

Supplementary Table S1. Statistics of RNA-Seq data.

Supplementary Table S2. Primers used in this study.

Funding

Data availability

The data that support the findings of this study are available from the corresponding author upon request.

References

Agrawal GK, Yamazaki M, Kobayashi M, Hirochika R, Miyao A, Hirochika H. Screening of the rice viviparous mutants generated by endogenous retrotransposon *Tos17* insertion. Tagging of a zeaxanthin epoxidase gene and a novel *ostatc* gene. Plant Physiol. 2001:**125**(3):1248–1257. https://doi.org/10.1104/pp.125.3.1248

Arsovski AA, Pradinuk J, Guo XQ, Wang S, Adams KL. Evolution of cis-regulatory elements and regulatory networks in duplicated genes of *Arabidopsis thaliana*. Plant Physiol. 2015:**169**(4):2982–2991. https://doi.org/10.1104/pp.15.00717

Barrero JM, Piqueras P, González-Guzmán M, Serrano R, Rodríguez PL, Ponce MR, Micol JL. A mutational analysis of the *ABA1* gene of

Arabidopsis thaliana highlights the involvement of ABA in vegetative development. J Exp Bot. 2005:**56**(418):2071–2083. https://doi.org/10.1093/jxb/eri206

Barrero JM, Rodríguez PL, Quesada V, Piqueras P, Ponce MR, Micol JL. Both abscisic acid (ABA)-dependent and ABA-independent pathways govern the induction of *NCED3*, *AAO3* and *ABA1* in response to salt stress. Plant Cell Environ. 2006:**29**(10):2000–2008. https://doi.org/10.1111/j.1365-3040.2006.01576.x

Chaudhary B, Flagel L, Stupar RM, Udall JA, Verma N, Springer NM, Wendel JF. Reciprocal silencing, transcriptional bias and functional divergence of homeologs in polyploid cotton (*Gossypium*). Genetics. 2009:**182**(2):503–517. https://doi.org/10.1534/genetics.109.102608

Chen K, Li GJ, Bressan RA, Song CP, Zhu JK, Zhao Y. Abscisic acid dynamics, signaling, and functions in plants. J Integr Plant Biol. 2020:**62**(1):25–54. https://doi.org/10.1111/jipb.12899

Clough SJ, Bent AF. Floral dip: a simplified method for Agrobacterium-mediated transformation of *Arabidopsis thaliana*. Plant J. 1998:**16**(6):735–743. https://doi.org/10.1046/j.1365-313x.1998.00343.x

Davuluri GR, van Tuinen A, Fraser PD, Manfredonia A, Newman R, Burgess D, Brummell DA, King SR, Palys J, Uhlig J, et al. Fruit-specific RNAi-mediated suppression of *DET1* enhances carotenoid and flavonoid content in tomatoes. Nat Biotechnol. 2005:**23**(7):890–895. https://doi.org/10.1038/nbt1108

Du H, Wang N, Cui F, Li X, Xiao J, Xiong L. Characterization of the beta-carotene hydroxylase gene *DSM2* conferring drought and oxidative stress resistance by increasing xanthophylls and abscisic acid synthesis in rice. Plant Physiol. 2010:**154**(3):1304–1318. https://doi.org/10.1104/pp.110.163741

Dun X, Zhou Z, Xia S, Wen J, Yi B, Shen J, Ma C, Tu J, Fu T. Bnac.Tic40, a plastid inner membrane translocon originating from *Brassica oleracea*, is essential for tapetal function and microspore development in *Brassica napus*. Plant J. 2011:**68**(3):532–545. https://doi.org/10.1111/j.1365-313X.2011.04708.x

Flagel LE, Wendel JF. Gene duplication and evolutionary novelty in plants. New Phytol. 2009:**183**(3):557–564. https://doi.org/10.1111/j.1469-8137.2009.02923.x

Force A, Lynch M, Pickett FB, Amores A, Yan YL, Postlethwait J. Preservation of duplicate genes by complementary, degenerative mutations. Genetics. 1999:**151**(4):1531–1545. https://doi.org/10.1093/genetics/151.4.1531

Galpaz N, Ronen G, Khalfa Z, Zamir D, Hirschberg J. A chromoplast-specific carotenoid biosynthesis pathway is revealed by cloning of the tomato white-flower locus. Plant Cell. 2006:**18**(8):1947–1960. https://doi.org/10.1105/tpc.105.039966

Galpaz N, Wang Q, Menda N, Zamir D, Hirschberg J. Abscisic acid deficiency in the tomato mutant *high-pigment* 3 leading to increased plastid number and higher fruit lycopene content. Plant J. 2008:**53**(5):717–730. https://doi.org/10.1111/j.1365-313X.2007.03362.x

Gayen D, Ali N, Sarkar SN, Datta SK, Datta K. Down-regulation of lipoxygenase gene reduces degradation of carotenoids of golden rice during storage. Planta. 2015:**242**(2):353–363. https://doi.org/10.1007/s00425-015-2314-4

Hauser F, Waadt R, Schroeder JI. Evolution of abscisic acid synthesis and signaling mechanisms. Curr Biol. 2011:**21**(9):R346–R355. https://doi.org/10.1016/j.cub.2011.03.015

He Y, Li M, Wang Y, Shen S. The R2R3-MYB transcription factor *MYB44* modulates carotenoid biosynthesis in *Ulva prolifera*. Algal Res. 2022:**62**:102578. https://doi.org/10.1016/j.algal.2021.102578

Hellens RP, Allan AC, Friel EN, Bolitho K, Grafton K, Templeton MD, Karunairetnam S, Gleave AP, Laing WA. Transient expression vectors for functional genomics, quantification of promoter activity and RNA silencing in plants. Plant Methods. 2005:**1**(1):13. https://doi.org/10.1186/1746-4811-1-13

Hieber AD, Bugos RC, Yamamoto HY. Plant lipocalins: violaxanthin de-epoxidase and zeaxanthin epoxidase. Biochim Biophys Acta. 2000:**1482**(1-2):84–91. https://doi.org/10.1016/S0167-4838(00)00141-2

Hoagland DR, Arnon DI. The water-culture method for growing plants without soil. Circular. California Agricultural Experiment Station. 1950:**347**:32. https://www.cabidigitallibrary.org/doi/full/10.5555/19500302257#core-collateral-purchase-access

Hu C, Lin SY, Chi WT, Charng YY. Recent gene duplication and sub-functionalization produced a mitochondrial GrpE, the nucleotide exchange factor of the Hsp70 complex, specialized in thermotolerance to chronic heat stress in Arabidopsis. Plant Physiol. 2012:**158**(2):747–758. https://doi.org/10.1104/pp.111.187674

Jaradat MR, Feurtado JA, Huang D, Lu Y, Cutler AJ. Multiple roles of the transcription factor AtMYBR1/AtMYB44 in ABA signaling, stress responses, and leaf senescence. BMC Plant Biol. 2013:**13**(1):192. https://doi.org/10.1186/1471-2229-13-192

Jefferson RA, Kavanagh TA, Bevan MW. GUS fusions: beta-glucuronidase as a sensitive and versatile gene fusion marker in higher plants. EMBO J. 1987:**6**(13):3901–3907. https://doi.org/10.1002/j.1460-2075.1987.tb02730.x

Jung C, Seo JS, Han SW, Koo YJ, Kim CH, Song SI, Nahm BH, Choi YD, Cheong JJ. Overexpression of *AtMYB44* enhances stomatal closure to confer abiotic stress tolerance in transgenic Arabidopsis. Plant Physiol. 2008:**146**(2):623–635. https://doi.org/10.1104/pp.107.110981

Kim JB, Kang JY, Kim SY. Over-expression of a transcription factor regulating ABA-responsive gene expression confers multiple stress tolerance. Plant Biotechnol J. 2004:**2**(5):459–466. https://doi.org/10.1111/j.1467-7652.2004.00090.x

Kranz HD, Denekamp M, Greco R, Jin H, Leyva A, Meissner RC, Petroni K, Urzainqui A, Bevan M, Martin C, et al. Towards functional characterisation of the members of the *R2R3-MYB* gene family from *Arabidopsis thaliana*. Plant J. 1998:**16**(2):263–276. https://doi.org/10.1046/j.1365-313x.1998.00278.x

Kumar S, Stecher G, Tamura K. MEGA7: molecular evolutionary genetics analysis version 7.0 for bigger datasets. Mol Biol Evol. 2016:**33**(7):1870–1874. https://doi.org/10.1093/molbev/msw054

Landt SG, Marinov GK, Kundaje A, Kheradpour P, Pauli F, Batzoglou S, Bernstein BE, Bickel P, Brown JB, Cayting P, et al. ChIP-seq guidelines and practices of the ENCODE and modENCODE consortia. Genome Res. 2012:**22**(9):1813–1831. https://doi.org/10.1101/gr.136184.111

Lee SY, Jang SJ, Jeong HB, Lee SY, Venkatesh J, Lee JH, Kwon JK, Kang BC. A mutation in *Zeaxanthin epoxidase* contributes to orange coloration and alters carotenoid contents in pepper fruit (*Capsicum annuum*). Plant J. 2021:**106**(6):1692–1707. https://doi.org/10.1111/tpj.15264

Lescot M, Déhais P, Thijs G, Marchal K, Moreau Y, Van de Peer Y, Rouzé P, Rombauts S. PlantCARE, a database of plant cis-acting regulatory elements and a portal to tools for in silico analysis of promoter sequences. Nucleic Acids Res. 2002:**30**(1):325–327. https://doi.org/10.1093/nar/30.1.325

Li F, Vallabhaneni R, Wurtzel ET. *PSY3*, a new member of the phytoene synthase gene family conserved in the Poaceae and regulator of abiotic stress-induced root carotenogenesis. Plant Physiol. 2008:**146**(3):1333–1345. https://doi.org/10.1104/pp.107.111120

Li LX, Wei ZZ, Zhou ZL, Zhao DL, Tang J, Yang F, Li YH, Chen XY, Han Z, Yao GF, et al. A single amino acid mutant in the EAR motif of *IbMYB44.2* reduced the inhibition of anthocyanin accumulation in the purple-fleshed sweetpotato. Plant Physiol Biochem. 2021:**167**:410–419. https://doi.org/10.1016/j.plaphy.2021.08.012

Liu R, Chen L, Jia Z, Lü B, Shi H, Shao W, Dong H. Transcription factor AtMYB44 regulates induced expression of the *ETHYLENE INSENSITIVE2* gene in Arabidopsis responding to a harpin protein. Mol Plant Microbe Interact. 2011:**24**(3):377–389. https://doi.org/10.1094/MPMI-07-10-0170

Liu Y, Lin-Wang K, Espley RV, Wang L, Li Y, Liu Z, Zhou P, Zeng L, Zhang X, Zhang J, et al. StMYB44 negatively regulates anthocyanin biosynthesis at high temperatures in tuber flesh of potato. J Exp Bot. 2019b:**70**(15):3809–3824. https://doi.org/10.1093/jxb/erz194

Liu Y, Ye S, Yuan G, Ma X, Heng S, Yi B, Ma C, Shen J, Tu J, Fu T, et al. Gene silencing of *BnaA09.ZEP* and *BnaC09.ZEP* confers orange color in *Brassica napus* flowers. Plant J. 2020:**104**(4):932–949. https://doi.org/10.1111/tpj.14970

Liu H, Zhu K, Tan C, Zhang J, Zhou J, Jin L, Ma G, Zou Q. Identification and characterization of *PsDREB2* promoter involved in tissue-specific expression and abiotic stress response from *Paeonia suffruticosa*. PeerJ. 2019a:**7**:e7052. https://doi.org/10.7717/peerj.7052

Lu S, Zhang Y, Zhu K, Yang W, Ye J, Chai L, Xu Q, Deng X. The citrus transcription factor CsMADS6 мodulates carotenoid metabolism by directly regulating carotenogenic genes. Plant Physiol. 2018:**176**(4):2657–2676. https://doi.org/10.1104/pp.17.01830

Luan Y, Chen Z, Tang Y, Sun J, Meng J, Tao J, Zhao D. Tree peony PsMYB44 negatively regulates petal blotch distribution by inhibiting dihydroflavonol-4-reductase gene expression. Ann Bot. 2023:**131**(2):323–334. https://doi.org/10.1093/aob/mcac155

Marin E, Nussaume L, Quesada A, Gonneau M, Sotta B, Hugueney P, Frey A, Marion-Poll A. Molecular identification of zeaxanthin epoxidase of *Nicotiana plumbaginifolia*, a gene involved in abscisic acid biosynthesis and corresponding to the ABA locus of *Arabidopsis thaliana*. EMBO J. 1996:**15**(10):2331–2342. https://doi.org/10.1002/j.1460-2075.1996.tb00589.x

Meng Y, Wang Z, Wang Y, Wang C, Zhu B, Liu H, Ji W, Wen J, Chu C, Tadege M, et al. The MYB activator WHITE PETAL1 associates with MtTT8 and MtWD40-1 to regulate carotenoid-derived flower pigmentation in *Medicago truncatula*. Plant Cell. 2019:**31**(11):2751–2767. https://doi.org/10.1105/tpc.19.00480

Moore RC, Purugganan MD. The evolutionary dynamics of plant duplicate genes. Curr Opin Plant Biol. 2005:**8**(2):122–128. https://doi.org/10.1016/j.pbi.2004.12.001

Nambara E, Marion-Poll A. Abscisic acid biosynthesis and catabolism. Annu Rev Plant Biol. 2005:**56**(1):165–185. https://doi.org/10.1146/annurev.arplant.56.032604.144046

Nguyen XC, Hoang MH, Kim HS, Lee K, Liu XM, Kim SH, Bahk S, Park HC, Chung WS. Phosphorylation of the transcriptional regulator MYB44 by mitogen activated protein kinase regulates Arabidopsis seed germination. Biochem Biophys Res Commun. 2012:**423**(4):703–708. https://doi.org/10.1016/j.bbrc.2012.06.019

Nisar N, Li L, Lu S, Khin NC, Pogson BJ. Carotenoid metabolism in plants. Mol Plant. 2015:**8**(1):68–82. https://doi.org/10.1016/j.molp.2014.12.007

Panchy N, Lehti-Shiu M, Shiu SH. Evolution of gene duplication in plants. Plant Physiol. 2016:**171**(4):2294–2316. https://doi.org/10.1104/pp.16.00523

Persak H, Pitzschke A. Tight interconnection and multi-level control of Arabidopsis MYB44 in MAPK cascade signalling. PLoS One. 2013:**8**(2):e57547. https://doi.org/10.1371/journal.pone.0057547

Rodriguez-Concepcion M, Avalos J, Bonet ML, Boronat A, Gomez-Gomez L, Hornero-Mendez D, Limon MC, Meléndez-Martínez AJ, Olmedilla-Alonso B, Palou A, et al. A global perspective on carotenoids: metabolism, biotechnology, and benefits for nutrition and health. Prog Lipid Res. 2018:**70**:62–93. https://doi.org/10.1016/j.plipres.2018.04.004

Sagawa JM, Stanley LE, LaFountain AM, Frank HA, Liu C, Yuan YW. An R2R3-MYB transcription factor regulates carotenoid pigmentation in *Mimulus lewisii* flowers. New Phytol. 2016:**209**(3):1049–1057. https://doi.org/10.1111/nph.13647

Simpson K, Fuentes P, Quiroz-Iturra LF, Flores-Ortiz C, Contreras R, Handford M, Stange C. Unraveling the induction of phytoene synthase 2 expression by salt stress and abscisic acid in *Daucus carota*. J Exp Bot. 2018:**69**(16):4113–4126. https://doi.org/10.1093/jxb/ery207

Song L, Huang SC, Wise A, Castanon R, Nery JR, Chen H, Watanabe M, Thomas J, Bar-Joseph Z, Ecker JR. A transcription factor hierarchy defines an environmental stress response

network. Science. 2016:**354**(6312):1550. https://doi.org/10.1126/science.aag1550

Stanley L, Yuan YW. Transcriptional regulation of carotenoid biosynthesis in plants: so many regulators, so little consensus. Front Plant Sci. 2019:**10**:1017. https://doi.org/10.3389/fpls.2019.01017

Sun T, Yuan H, Cao H, Yazdani M, Tadmor Y, Li L. Carotenoid metabolism in plants: the role of plastids. Mol Plant. 2018:**11**(1):58–74. https://doi.org/10.1016/j.molp.2017.09.010

Tanaka Y, Sasaki N, Ohmiya A. Biosynthesis of plant pigments: anthocyanins, betalains and carotenoids. Plant J. 2008:**54**(4):733–749. https://doi.org/10.1111/j.1365-313X.2008.03447.x

Toledo-Ortiz G, Johansson H, Lee KP, Bou-Torrent J, Stewart K, Steel G, Rodríguez-Concepción M, Halliday KJ. The HY5-PIF regulatory module coordinates light and temperature control of photosynthetic gene transcription. PLoS Genet. 2014:**10**(6):e1004416. https://doi.org/10.1371/journal.pgen.1004416

Uno Y, Furihata T, Abe H, Yoshida R, Shinozaki K, Yamaguchi-Shinozaki K. Arabidopsis basic leucine zipper transcription factors involved in an abscisic acid-dependent signal transduction pathway under drought and high-salinity conditions. Proc Natl Acad Sci USA. 2000:**97**(21):11632–11637. https://doi.org/10.1073/pnas.190309197

Wang Z, Li X, Yao X, Ma J, Lu K, An Y, Sun Z, Wang Q, Zhou M, Qin L, et al. MYB44 regulates PTI by promoting the expression of *EIN2* and *MPK3/6* in Arabidopsis. Plant Commun. 2023:**4**(6):100628. https://doi.org/10.1016/j.xplc.2023.100628

Wang Z, Su G, Li M, Ke Q, Kim SY, Li H, Huang J, Xu B, Deng XP, Kwak SS. Overexpressing Arabidopsis *ABF3* increases tolerance to multiple abiotic stresses and reduces leaf size in alfalfa. Plant Physiol Biochem. 2016:**109**:199–208. https://doi.org/10.1016/j.plaphy.2016.09.020

Xing HL, Dong L, Wang ZP, Zhang HY, Han CY, Liu B, Wang XC, Chen QJ. A CRISPR/Cas9 toolkit for multiplex genome editing in plants. BMC Plant Biol. 2014:**14**(1):327. https://doi.org/10.1186/s12870-014-0327-y

Yang Y, Li HG, Wang J, Wang HL, He F, Su Y, Zhang Y, Feng CH, Niu M, Li Z, et al. ABF3 enhances drought tolerance via promoting ABA-induced stomatal closure by directly regulating *ADF5* in *Populus euphratica*. J Exp Bot. 2020:**71**(22):7270–7285. https://doi.org/10.1093/jxb/eraa383

Yang J, Zhang J, Wang Z, Zhu Q, Wang W. Hormonal changes in the grains of rice subjected to water stress during grain filling. Plant Physiol. 2001:**127**(1):315–323. https://doi.org/10.1104/pp.127.1.315

Ye S, Hua S, Ma T, Ma X, Chen Y, Wu L, Zhao L, Yi B, Ma C, Tu J, et al. Genetic and multi-omics analyses reveal *BnaA07.PAP2*$^{In-184–317}$ as the key gene conferring anthocyanin-based color in *Brassica napus* flowers. J Exp Bot. 2022:**73**(19):6630–6645. https://doi.org/10.1093/jxb/erac312

Yoo SD, Cho YH, Sheen J. Arabidopsis mesophyll protoplasts: a versatile cell system for transient gene expression analysis. Nat Protoc. 2007:**2**(7):1565–1572. https://doi.org/10.1038/nprot.2007.199

Yoshida T, Mogami J, Yamaguchi-Shinozaki K. ABA-dependent and ABA-independent signaling in response to osmotic stress in plants. Curr Opin Plant Biol. 2014:**21**:133–139. https://doi.org/10.1016/j.pbi.2014.07.009

Zhang H, Hu Y, Gu B, Cui X, Zhang J. VaMYB44 transcription factor from Chinese wild *Vitis amurensis* negatively regulates cold tolerance in transgenic *Arabidopsis thaliana* and *V. vinifera*. Plant Cell Rep. 2022:**41**(8):1673–1691. https://doi.org/10.1007/s00299-022-02883-w

Zhang B, Liu C, Wang Y, Yao X, Wang F, Wu J, King GJ, Liu K. Disruption of a *CAROTENOID CLEAVAGE DIOXYGENASE 4* gene converts flower colour from white to yellow in *Brassica* species. New Phytol. 2015:**206**(4):1513–1526. https://doi.org/10.1111/nph.13335

Zong W, Tang N, Yang J, Peng L, Ma S, Xu Y, Li G, Xiong L. Feedback regulation of ABA signaling and biosynthesis by a bZIP transcription factor targets drought-resistance-related genes. Plant Physiol. 2016:**171**(4):2810–2825. https://doi.org/10.1104/pp.16.00469

Zou C, Lehti-Shiu MD, Thomashow M, Shiu SH. Evolution of stress-regulated gene expression in duplicate genes of *Arabidopsis thaliana*. PLoS Genet. 2009:**5**(7):e1000581. https://doi.org/10.1371/journal.pgen.1000581